4-20-2023

The miR167-OsARF12 module regulates grain filling and grain size downstream of miR159

Yafan Zhao
Henan Agricultural University

Xiaofan Zhang
Shanghai Jiao Tong University

Yuan Cheng
Henan Agricultural University

Xiangxiang Du
Henan Agricultural University

Sachin Teotia
Sharda University

See next page for additional authors

Recommended Citation

Zhao, Y., Zhang, X., Cheng, Y., Du, X., Teotia, S., Miao, C., Sun, H., Fan, G., Tang, G., Xue, H., Zhao, Q., & Peng, T. (2023). The miR167-OsARF12 module regulates grain filling and grain size downstream of miR159. *Plant communications*, 100604. http://doi.org/10.1016/j.xplc.2023.100604
Retrieved from: https://digitalcommons.mtu.edu/michigantech-p/17095

Journal Pre-proof

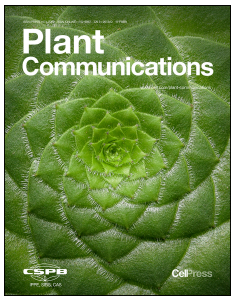

The *miR167-OsARF12* module regulates grain filling and grain size downstream of *miR159*

Yafan Zhao, Xiaofan Zhang, Yuan Cheng, Xiangxiang Du, Sachin Teotia, Chunbo Miao, Huwei Sun, Guoqiang Fan, Guiliang Tang, Hongwei Xue, Quanzhi Zhao, Ting Peng

PII: S2590-3462(23)00115-3

DOI: https://doi.org/10.1016/j.xplc.2023.100604

Reference: XPLC 100604

To appear in: *PLANT COMMUNICATIONS*

Received Date: 14 October 2022

Revised Date: 20 March 2023

Accepted Date: 18 April 2023

Please cite this article as: Zhao, Y., Zhang, X., Cheng, Y., Du, X., Teotia, S., Miao, C., Sun, H., Fan, G., Tang, G., Xue, H., Zhao, Q., Peng, T., The *miR167-OsARF12* module regulates grain filling and grain size downstream of *miR159*, *PLANT COMMUNICATIONS* (2023), doi: https://doi.org/10.1016/j.xplc.2023.100604.

The *miR167-OsARF12* module regulates grain filling and grain size downstream of *miR159*

Yafan Zhao[1,2,3], Xiaofan Zhang[4], Yuan Cheng[1,2,3], Xiangxiang Du[1,2,3], Sachin Teotia[5], Chunbo Miao[1,2,3], Huwei Sun[1,2,3], Guoqiang Fan[6], Guiliang Tang[7], Hongwei Xue[4*], Quanzhi Zhao[1,2,3,8*] and Ting Peng[1,2,3*]

[1] Collaborative Innovation Center of Henan Grain Crops, Henan Agricultural University, Zhengzhou 450002, China

[2] Key Laboratory of Rice Biology in Henan Province, Henan Agricultural University, Zhengzhou 450002, China

[3]Henan Engineering Laboratory of Rice, Henan Agricultural University, Zhengzhou 450002, China

[4]Joint Center for Single Cell Biology/School of Agriculture and Biology, Shanghai Jiao Tong University, Shanghai 200240, China

[5] Department of Biotechnology, Sharda University, Greater Noida, 201306, India

[6] Institute of Paulownia, Henan Agricultural University, Zhengzhou, Henan 450002, China

[7]Department of Biological Sciences, Michigan Technological University, Houghton, MI 49931, USA

[8]College of Agriculture, Guizhou University, 550025, China

Correspondence: Ting Peng (lypengting@163.com), Quanzhi Zhao (qzzhaoh@126.com), Hongwei Xue (hwxue@sjtu.edu.cn).

Short Summary: Plant miRNAs are gradually becoming new targets for cultivating excellent grain size and yield. This study shows that *miR167-OsARF12* is thought to be regulated by *miR159* through OsGAMYBL2 to control grain filling and grain size. *OsCDKF;2* targeted by *OsARF12* mediates auxin and BR signals and involves in cell cycle process, resulting in increased grain filling.

ABSTRACT

Grain weight and quality are always determined by the grain filling. Plant miRNAs have drawn attention as key targets for regulating grain size and yield. Yet the mechanisms underlying the regulation of grain size are largely unclear due to the complex networks controlling this trait. Our earlier studies proved that the suppressed expression of *miR167* (*STTM*/*MIM167*) substantially increased grain weight. In a field test, the increased yield up to 12.90%-21.94% due to the significantly enhanced grain filling rate. Biochemical and genetic analyses reveal the regulatory effects of *miR159* on *miR167* expression. Further analysis indicates that *OsARF12* is the major mediator of *miR167* in regulating rice grain filling. Expectedly, over expressing *OsARF12* could resemble the phenotype of *STTM/MIM167* plants with respect to grain weight and grain filling rate. Upon in-depth analysis, we found that OsARF12 activates *OsCDKF;2* expressions by directly binding to the TGTCGG motif in the promoter region. Flow cytometric analysis in young panicles of plants overexpressing *OsARF12* and cell number examination of *cdkf;2* mutants verify that *OsARF12* positively regulates grain filling and grain size by targeting *OsCDKF;2*. Moreover, RNA-seq result suggests that *miR167*-*OsARF12* module is involved in the cell development process and hormone pathways. Additionally, plants overexpressing *OsARF12* or *cdkf;2* mutants present enhanced or reduced sensitivity to exogenous auxin and brassinosteroid (BR) treatments, confirming that *OsCDKF;2* targeting by *OsARF12* mediates auxin and BR signaling. Our results reveal that *miR167*-*OsARF12* module works downstream of miR159 to regulate rice grain filling and grain size by *OsCDKF;2* through controlling cell division and mediating auxin and BR signals.

Key words: rice, *miR167*, *OsARF12*, *OsCDKF;2*, grain filling, cell cycle

INTRODUCTION

Feeding the ever-growing global population remains a major challenge in the field of agriculture (Mcdonald, 2012). It is crucial to increase crop productivity through efficient breeding and biotechnology. Rice, which constitutes a staple food for approximately 50% of the global population (Rosegrant and Cline, 2003), relies on three major factors to determine its grain yield- the number of panicles per plant, effective grain number per panicle, and grain weight. The number of panicles per plant, effective grain number per panicle and grain weight are generally considered to be the decisive factors controlling grain yield. Rice grain filling and plumpness significantly influence

grain weight and quality (Zhou et al., 2013). Recent advances have identified several signaling pathways that control grain weight and yield through maternal tissues. Some of these pathways include or involve the ubiquitin-proteasome pathway, G-protein signaling, mitogen-activated protein kinase (MAPK) signaling, phytohormone perception and homeostasis, and some transcriptional regulators (Li et al., 2019). Consequently, the molecular mechanisms underlying the rice yield-related regulatory networks remain elusive. Therefore, comprehending the mechanisms controlling grain weight and yield remains an essential research field in plant science.

MicroRNAs (miRNAs), which refer to a class of short noncoding RNAs, have been established as key targets for regulating plant development by negatively regulating their downstream targets at the post-transcriptional or translational levels (Bartel, 2009). Plant hormones, including brassinosteroid (BR) and auxin, play important role in regulating rice seed size and grain weight by controlling cell division or expansion (Hu et al., 2018; Wu et al., 2016; Zhao et al., 2018). ABA may regulate rice grain filling by affecting sucrose starch signaling in a dose-dependent manner (Zhu et al., 2011). Recently, several studies have focused on the network between miRNAs and agronomic traits, including grain weight and yield of crop plants, by mediating phytohormones signals (Peng et al., 2019). *OsmiR397* is the first reported miRNA that positively controls rice seed size and grain yield by downregulating its target *OsLAC*, which is involved in plant sensitivity to BR (Zhang et al., 2013). The *osmiR396-OsGRF4* regulatory module which might be involved in BR signaling through the promotion of cell expansion and cell proliferation has been a typical case for seed size determination and grain yield improvement (Duan et al., 2015; Hu et al., 2015; Tong et al., 2012). Rice miRNA *osmiR1848* targets the obtusifoliol 14α-demethylase gene *OsCYP51G3* and mediates the biosynthesis of phytosterols and brassinosteroids in seed size and quality regulation (Xia et al., 2015). The *osmiR159d-OsGAMYBL2* pair functions as an early BR-responsive module regulating the expression of BU1, a BR-regulated gene, to control grain size (Gao et al., 2018). Suppression of *osmiR1432* or overexpression of its cleavage-resistant target, *OsACOT,* significantly increases the IAA and ABA content in the endosperm, leading to the improvement of grain weight and yield through increased grain filling rate (Zhao et al., 2019a).

Although many miRNAs regulating grain size and weight have been reported, still new factors might be involved in this comprehensive process. Moreover, the coordination among various small

RNAs helps modulate specific development processes. For example, the *miR156-SPL9-miR172* regulatory pathway is responsible for regulating the transition from vegetative to reproductive phase (Wang, 2014). *miR159* functions upstream of *miR156* to modulate vegetative phase change in *Arabidopsis* (Guo et al., 2017). Most recently, *OsmiR396-OsGRF8* modulates rice grain size by directly regulating embryo-specific *miR408* (Yang et al., 2021). Whether there is any other coordination between miRNAs controlling grain size and weight, remains elusive.

Auxin response factors (ARFs) are transcription factors that bind to auxin-responsive elements (AuxREs) located within the promoter regions of early auxin-responsive genes and mediate auxin signal transduction to regulate the growth and development of plants (Weijers and Friml, 2009). *Arabidopsis* contains 23 ARF genes while rice has 25 (Wang et al., 2007). Notably, several ARF genes have been identified as the cleavage targets of *miR167*, a conserved miRNA in plants. In *Arabidopsis*, *AtARF6* and *AtARF8* have been confirmed as the direct targets of *miR167* in maternal control of embryonic and seed development, as well as anther growth (Yao et al., 2019). In rice, a model monocotyledonous plant species, *OsARF6* and *OsARF12* were predicted as the targets of *miR167* in earlier studies (Rhoades et al., 2002), and later research found that *OsARF17* and *OsARF25* are also direct targets of *miR167* in rice (Liu et al., 2012). Furthermore, the *miR167*-ARFs module plays an important role in various aspects of rice growth and development. Previous studies reported that four ARFs (*OsARF6/12/17/25*) downregulated by *miR167* are associated with rice growth and development, and overexpression of *miR167* results in growth and developmental defects in transgenic plants (Liu et al., 2012). Other research revealed that *OsmiR167-OsARF8-GH3* respond to exogenous auxin in cultured rice cells provides evidence of miRNA-mediated auxin signaling (Yang et al., 2006). *OsmiR167d-OsARF12* module regulates root elongation and affects iron accumulation in rice (Qi et al., 2012b) while *Osa-miR167d* negatively regulates rice immunity by down-regulating *OsARF12* to facilitate the infection of *M.oryzae* (Zhao et al., 2019b). And the most recent studies indicate that *OsmiR167a* represses *OsARF12*, *OsARF17* and *OsARF25* to control rice tiller angle by fine-tuning auxin asymmetric distribution in shoots (Li et al., 2020). However, it is still unclear how the *OsmiR167-OsARFs* module regulates rice grain weight and yield, which requires further investigation.

In previous study, we identified a set of miRNAs differentially expressed in superior and inferior

grains during rice grain filling. Among them, all of the members of the *Osa-miR167* family showed a relatively high expression level. More remarkably, *miR167* expression was higher in superior grains than in inferior grains during the early stage, while it followed an opposite trend during the late stage of grain filling (Peng et al., 2011; Peng et al., 2014). Furthermore, suppressing the expression of *miR167* by STTM (short tandem target mimic) under the Gt13a promoter significantly increased 1,000-hulled grain weight (Peng et al., 2018). In this study, we explored the role of *miR167* in rice grain filling regulation and seed size determination. Besides STTM, we also generated transgenic rice downregulating OsmiR167 via MIM (target mimicry). In addition, we discovered the direct regulatory effects of *miR159* on the expression of *miR167*. *OsARF12* was examined as the main target of miR167 in rice grain filling. Both *miR167* underexpressing plants and *OsARF12* overexpressing plants exhibited an increase grain filling rate, grain weight and yield. Moreover, cyclin-dependent kinase, *OsCDKF;2,* was confirmed as the direct downstream target of OsARF12 and knock out *OsCDKF;2* displayed reduced grain filling and grain size. Our findings indicate that miR167-*OsARF12* module regulates rice yield via *OsCDKF;2* and downstream of miR159.

RESULTS

Suppressed expression of *miR167* enhances grain weight by accelerating grain filling rate

To elucidate the function of *miR167* in rice grain filling, vectors under endosperm-specific promoter (Gt13a) were constructed to drive the expression of *STTM167* and *MIM167* (Supplemental Figure 1). Stem-loop PCR showed significantly decreased expression of *miR167* in both *STTM167* plants and *MIM167* plants (Figure 1C). We observed yield-related phenotypes in *STTM/MIM167* plants such as grain size and features of the main panicle. Compared with the wild-type (WT), *STTM/MIM167* plants displayed bigger grain size and heavier 1,000 hulled grain weight and slightly more branch number (Figure 1A and Figure 1B and Figure 1D and Supplemental S2 and Supplemental Table 1). However, there was a slight difference to concerning branch numbers among plants from different years (Supplemental Table 2). Further analysis of grain characteristics revealed an obvious increase in grain length and width in *STTM/MIM167* plants (Figure 1E and Figure 1F). Specifically, the degree of increase of grain length and width was approximately 10.17% ($P<0.01$) and 11.42% ($P<0.01$) compared with WT plants, respectively. However, the length/width ratio, it showed no significant difference between WT and *miR167* transgenic lines (Supplemental Table 2).

Given the importance of grain filling to grain weight and yield, a time course measurement of dry 1,000-grain weight of filling grains was conducted (Figure 1H), revealing an increase in the filling rate in *STTM167/MIM167* plants (Figure 1I and Figure 1J), implying the potential role of miR167 in grain filling regulation. Filling parameters including maximum and mean filling rate were fitted and calculated by Richards' equation. Interestingly, compared with wild type, the maximum filling rate got significantly increased by 17.71%-25.14% (P<0.01) in the *STTM167* plants and by 11.43%-32.57% (P<0.01) in the *MIM167* plants. In addition, average filling rate in *STTM167* plants and *MIM167* plants also increased by 18.33%-25.83% (P<0.01) and 11.67%-33.33% (P<0.01), respectively (Supplemental Table 1). Finally, the true yield of *STTM/MIM167* plants under a field trial showed a 12.22%-25.61% (P<0.01) improvement over that of WT plants (Figure 1G). These results demonstrated that suppressed expression of *miR167* in grain promotes rice grain filling rate to increase seed plumpness and yield.

Genetic interaction and regulatory effect of *miR159-GAMYBL2* on *miR167*

miR159 positively regulates grain size, and *miR167* and *OsGAMYBL2* negatively regulate it. Moreover, there are multiple MYB-binding sites in the promoter region of *MIR167* loci (Supplemental Figure 3A), which made us wonder whether there is any genetic interaction between *miR159* and *miR167*. To figure this out, we crossed the *STTM159* plants with *STTM167-17* plants and amplified specific sequences from parental and progeny plants with varying lengths (Figure 2A). The F2 plants showed an average grain size of *STTM159* and *STTM167-17* (Figure 2B), with grain length, grain width and 1,000-grain weight displaying mean values of the two parents (Figure 2C and Figure 2D and Figure 2E), indicating that *STTM167-17* could partially complement the decreased grain size of *STTM159*. We hypothesized that the complementation of *STTM159* phenotypes by *STTM167* to concerning grain size and weight was caused by the upregulation of *miR167* in *STTM159* plants. The expression of *miR167* in *STTM159* plants was verified by small RNA sequencing and stem-loop qRT-PCR. As expected, the expression of *miR167* was significantly upregulated in *STTM159* roots, shoots, and grains (Figure 2E and Figure 2F and Figure 2G). This explains why *STTM167* complemented *STTM159* phenotypes.

We speculated that *miR159* regulates *miR167* through *OsGAMYBL2*, the direct target of miR159 . Additionally, the molecular basis for the genetic interaction between *miR159* and *miR167* might

involve the transcriptional regulation of *miR167* by *OsGAMYBL2*. Therefore, we analyzed the possible regulatory effects of *OsGAMYBL2* on the expression of *miR167*. Further analysis indicated that the potential binding motifs contained in the *miR167e* and *miR167h* promoters cover most OsGAMYBL2 binding sites. Then we initially synthesized *miR167e* and *miR167h* binding motifs in tandem, and then preliminarily verified the interaction between the predicted binding motifs and OsGAMYBL2 by yeast one hybrid (Y1H). Y1H results showed that the predicted tandem motifs tandem in the *miR167h* promoter could interact with OsGAMYBL2, while the predicted tandem motif in the *miR167e* promoter could not (Supplemental Figure 3B). Based on this, we selected the promoter of *miR167h* to explore the interaction between *miR167* and OsGAMYBL2. We then divided the promoter region of *miR167h* into four fragments containing MYB-binding sites (h1-h4) and one fragment without a MYB-binding motif (h0) and found that MYB-binding motifs in the *miR167h2* region were able to bound by OsGAMYBL2 in yeast cells (Figure 2H and Supplemental Figure 3C). These results suggested that *OsGAMYBL2* might be the upstream regulator of *miR167*. The enrichment of fragments containing putative MYB-binding motifs of *miR167h* promoter was analyzed by ChIP-qPCR, which was performed with the *OsGAMYBL2-Flag* lines. As shown in Figure 2L, fragment h2 was obviously enriched in the *OsGAMYBL2-Flag* lines (Figure 2L). These results further indicated that OsGAMYBL2 binds to the motifs in the h2 region of *miR167* promoter. We subsequently conducted transient expression assays to confirm the *in vivo* result. The strains harboring the *35S::OsGAMYBL2* effector and *OsmiR167::LUC* reporter plasmids were co-transformed into rice protoplasts and *N. benthamiana* leaf epidermal cells, respectively. The LUC activity was examined after 14h and 48h incubation in darkness. The co-expression of *35S::OsGAMYBL2* and *OsmiR167::LUC* significantly increased the activity of luciferase when compared with the effects of the empty vector control (Figure 2I and Figure 2J and Figure 2K), indicating the transcriptional activation by *OsGAMYBL2* on the promoter of *miR167*.

***OsARF12* was validated as the main target of *miR167* in rice grain filling**

In plants, miRNAs exert their functions by inhibiting the expression of their target genes. Accordingly, it is essential to identify the downstream target(s) of *miR167* to understand its regulatory function in influencing grain weight and yield. It has been reported that *OsARF6*, *OsARF12*, *OsARF17* and *OsARF25* are the direct downstream cleavage targets of *miR167* (Li et al.,

2020; Liu et al., 2012). To investigate the main target of *miR167* in regulating grain filling, spatiotemporal expression patterns of *miR167* and its four targets in various rice organs including roots, leaves, stems, panicles and developing grains at different growth stages were firstly determined by qRT-PCR (Figure 3A, Supplemental Figure 4). All of the four targets exhibited different antagonistic expression patterns concerning miR167. During the process of grain development, the expression of *OsARF12* achieved the highest level among the four targets and its expression gradually increased over time (Figure 3A). Furthermore, expression levels of the four targets in developing grains of *STTM/MIM167* plants were detected by qRT-PCR. As shown in Figure S4, similar to the results of the expression pattern of the four targets, *OsARF12* had the highest expression level (Supplemental Figure 5). More importantly, the expression level of *OsARF12* was upregulated during the whole grain development stage in *STTM/MIM167* plants compared with WT plants (Supplemental Figure 5). Considering the antagonistic expression pattern of *OsARF12* to that of *miR167*, we suggested that *OsARF12* could be the likely main target of *miR167* influencing grain filling.

To explore our hypothesis, a phylogenetic tree was also constructed using protein sequences of the four targets. The analysis showed that OsARF6 and OsARF17 had the highest homology and were more similar to OsARF25, whereas all of these three presented a relative low homology with OsARF12(Supplemental Figure 6A). Meanwhile, transgenic plants overexpressing *OsARF6*, *OsARF12*, *OsARF17* and *OsARF25* (named as *ARF6 OE*, *ARF12 OE*, *ARF17 OE*, *ARF25 OE*, respectively) under a constitutive promoter were generated. Phenotypic analysis showed that 1,000-grain weight of the transgenic plants of the four targets increased except in very few transgenic lines in varying degrees compared with WT plants. Among the transgenic lines, *ARF12 OE* plants got the heaviest grain weight (Figure 3B and Figure 3C and Figure 3D and Supplemental Figure 6B and Supplemental Figure 6C). Furthermore, expression of *OsARF12* had a significant positive correlation with varying grain weights, implying that the dosage of the *OsARF12* mRNA contributed to grain weight (Figure 3E). These results indicated that *OsARF12* was the main target of *miR167* in rice grain filling regulation.

OsARF12 positively regulates rice grain filling and weight through promoting cell division

It has been reported that OsARF12 is a transcriptional activator (Qi et al., 2012b). To study the

subcellular localization of OsARF12, an OsARF12-eGFP fusion protein was constructed under the control of the constitutive Cauliflower mosaic virus (CaMV)-35S promoter. During the transient expression of the fusion protein in rice protoplasts, green fluorescence was visible throughout the cytoplasm in protoplasts with the *35S::eGFP* control plasmid. The results confirmed the localization of OsARF12 in the nucleus (Figure 4A), which was in accord with the localization of transcription factors, in general.

To check whether *miR167*-mediated negative regulation of *OsARF12* influences grain weight and yield, we hypothesized that overexpression or suppressed expression of *OsARF12* in rice would lead to an increase or decrease in grain weight and filling rate, respectively. Therefore, besides *ARF12 OE* plants, transgenic plants with reduced expression of *OsARF12* through RNA interference (*ARF12 RNAi*) driven by endosperm-specific expression promoter Gt13a were also created. The relative expression level of *OsARF12* in *ARF12 OE* and *ARF12 RNAi* plants were firstly determined by qRT-PCR. As expected, the mRNA expression level of *OsARF12* increased and decreased significantly in the developing grains of *ARF12 OE* and *ARF12 RNAi* plants when compared with WT plants (Figure 4D). However, expressions of *OsARF6*, *OsARF17* and *OsARF25* remained approximately unchanged compared with WT plants (Supplemental Figure 7B). Because *miR167* was found to promote grain weight and filling rate, we subsequently evaluated the effects of *OsARF12* on the traits of grains and grain filling parameters. Notably, the grain size of *ARF12 OE* or *ARF12 RNAi* plants was larger or smaller compared to WT (Figure 4B and Figure 4C and Supplemental Figure 7C and Supplemental Figure 7D). Moreover, the 1,000-grain weight of *ARF12 OE* was 27.87g-28.73g, which had an increase by 12.37%-15.86% ($P<0.01$) compared with 24.80g of WT (Figure 4E). Detailed analysis of grain traits showed that there was a 6.68%-9.70% ($P<0.01$) and 2.77%-3.52% ($P<0.01$), respectively (Figure 4F and Figure 4G) improvement in grain length and grain width in *ARF12 OE*. In contrast, the 1,000-grain weight of *ARF12 RNAi* decreased approximately 4.84%-6.18% ($P<0.01$) compared with WT (Figure 4E), with a reduction of grain length was up to 0.02 mm per grain ($P<0.01$) and grain width reduced by 2.85%-6.67% ($P<0.01$) (Figure 4F and Figure 4G). Taken together, these findings demonstrate that grain size and weight vary inversely with the expression level of *OsARF12*. Therefore, to a certain degree, *OsARF12* plays a positive role in the regulation and determination of grain size and weight.

Similarly, 1,000-grain weight during the filling stage of *ARF12 OE* plants and *ARF12 RNAi* plants were measured and filling parameters were calculated. Notably, when compared with WT, grain weight, average filling rate and maximum filling rate in *ARF12 OE* plants substantially increased (Figure 4I and Figure 4J and Figure 4K). Specifically, the maximum and average filling rate in *ARF12 OE* plants increased by 7.36%-10.43% (P<0.01) and 3.39%-5.08% (P<0.01), respectively, whereas they decreased by 4.91%-10.43% (P<0.01) and 16.10%-22.03% (P<0.01) in *ARF12 RNAi* plants in contrast (Supplemental Table 4). Meanwhile, the number of primary and secondary branches, length of panicle and number of effective grains per panicle in *ARF12 OE* or *ARF12 RNAi* plants showed no significant difference from those in the WT plants (Supplemental Figure 7A and Supplemental Table 4). Finally, in a field test evaluating the yield of *ARF12 OE* and *ARF12 RNAi* transgenic plants, the results indicated that the degree of yield change was 19.29% to 23.07% (P<0.01) and -17.53% to -21.33% (P<0.01), respectively (Figure 4H).

We subsequently investigated the cellular mechanism underlying *OsARF12*- mediated modulation of grain size in rice. We hypothesized that the increased rate of cell division may be responsible for larger grain size of *ARF12 OE* plants. Therefore, we determined the cell division rate of young panicles from both WT and *ARF12 OE* plants using flow cytometry. Measurement of DNA contents in the cells of the young panicle showed that the percentage of S and G2/M phase cells with higher DNA content was elevated in *ARF12 OE* plants, whereas the percentage of G1 phase with 2C DNA content after new cell cycles were initiated compared with WT (Figure 4L and Figure 4M). Thus, it can be inferred from our results that *OsARF12* positively promotes cell division to improve grain development and yield by influencing rice grain filling.

OsARF12 directly binds to the promoter region of *OsCDKF;2*

To explore the downstream target of OsARF12 in rice grain filling, up-regulated genes in *ARF12 OE* plants in comparison with wild type were initially screened. At the same time, scoring matrix analysis was used to predict the binding elements of OsARF12 and the TGTCGG element was selected as the promising binding sequence (Figure 5A). Then all -2.0 kb upstream promoter regions of genes including the TGTCGG element with up-regulated expression in *ARF12 OE* plants were screened successfully. Based on our findings of an increased cell division rate in *ARF12 OE* young panicles by flow cytometry, we postulated *OsARF12* controls grain filling and yield by regulating

cell division through its downstream target. Therefore, we focused on *OsCDKF;2* (*Os12g0424700*), which is predicted to be involved in cell cycle, was selected as the prospective target of *OsARF12* in grain filling and yield regulation. To ascertain the direct binding of OsARF12 to *OsCDKF;2* promoter, yeast one-hybrid assay was conducted. The data revealed that OsARF12 could bind the predicted site in the promoter region of *OsCDKF;2* (Figure 5C and Figure 5D and Supplemental Figure 8). To further confirm OsARF12 binding on the promoter of *OsCDKF;2 in vivo,* we carried out ChIP-qPCR in grains and spikelets through the anti-FLAG antibody against OsARF12 compared to the control IgG. The element-containing DNA was significantly enriched in spikelet and young panicle of *ARF12 OE* plants (Figure 5F and Figure 5G). Altogether, our findings strongly indicated that OsARF12 binds to the promoter region of *OsCDKF;2*.

To determine the regulatory role of OsARF12 on *OsCDKF;2* expression, we examined *OsCDKF;2* transcript levels in both in *ARF12 OE* and *ARF12 RNAi* plants. The analyses revealed that *OsCDKF;2* transcripts exhibited enhanced accumulation in the *ARF12 OE* plants, but were reduced in *ARF12 RNAi* plants relative to wild type (Figure 5B). These results implied that the expression of *OsCDKF;2* is positively correlated with that of *OsARF12*. To further validate this correlation *in vivo*, we performed transient expression assays in rice protoplasts by co-transforming strains harboring a *35S::OsARF12* effector and *OsCDKF;2::LUC* reporter plasmids. The LUC activity was examined after14h incubation in darkness. The co-expression of *35S::OsARF12* and *OsCDKF;2::LUC* sharply increased the activity of luciferase when compared with the effects of the empty vector control (Figure 5E). This result supported the conclusion that OsARF12 positively regulates *OsCDKF*;*2* expression *in vivo* by directly binding to the promoter region.

OsCDKF;2 plays a positive role in grain filling regulation

To confirm if *OsCDKF;2* was responsible for *OsARF12*-mediated regulation of rice grain size and weight, single-guide RNA targeting the *OsCDKF;2* locus (sgRNA; bases 72-91 from the ATG start codon in the cDNA) constructs were generated and introduced into rice using CRISPR/Cas9 (Supplemental Figure 9A). Three *cdkf;2* mutants (*cdkf-1*, 1-base A insertion; *cdkf-8*, 1-base T insertion; *cdkf-13*, 1-base G deletion and CG to GT) with wild type (WT) background and two *ARF12 OE-cdkf;2* mutants *(ARF12 OE-cdkf;2-21*, 1-base T insertion; *ARF12 OE-cdkf;2-27*, 1-base A insertion) with *ARF12 OE* background were generated and their grain traits were investigated

(Supplemental Figure 9B). *OsCDKF;2* expression was downregulated in the different mutant lines compared with WT and *ARF12 OE* plants, respectively (Supplemental Figure 9C). However, expression of *OsARF12* in *ARF12 OE-cdkf;2* mutants was still markedly increased compared with WT (Supplemental Figure 9D). As expected, grains of the three *cdkf;2* mutants or the two *ARF12 OE-cdkf;2* mutants showed a significant reduction in size compared to the respective controls (Figure 6A). The 1,000-grain weight of *cdkf;2* mutants or *ARF12 OE-cdkf;2* mutants reduced by 26.53%-47.85% (P<0.01) or by 25.45%-32.12% (P<0.01) compared with WT and *ARF12 OE* plants, respectively (Figure 6B). Detailed analysis of grain traits showed that the decreased degree of grain length, grain width and grain thickness in *cdkf;2* mutants was 7.39%-13.31% (P<0.01), 10.14%-19.41(P<0.01) and 3.03%-15.24% (P<0.01), respectively, compared with WT (Figure 6C and Figure 6D and Figure 6E). Similarly, the reduction of grain length, grain width and grain thickness in *ARF12 OE-cdkf;2* mutants was 9.10%-9.75% (P<0.01), 14.86%-16.55% (P<0.01) and 8.43%-16.11% (P<0.01), respectively, compared with *ARF12 OE* plants (Figure 6C and Figure 6D and Figure 6E).

Grain filling is a critical determinant of grain size and grain weight. We conducted a temporal measurement of grain filling rate during the whole filling stage, indicating that *cdkf;2* and *ARF12 OE-cdkf;2* mutants had a significant decrease of grain filling rate during early and middle filling stage compared with WT and *ARF12 OE* plants, respectively (Figure 6F and Figure 6G). Especially, the maximum filling rate of *cdkf;2* and *ARF12 OE-cdkf;2* mutants reduced by 13.59%-33.12% and 14.79%-23.03% compared with their individual control. We then investigated the cellular mechanism underlying *OsCDKF;2* modulation grain size by detecting the cross-sections of the central parts of the grain spikelet hulls before heading stage. Interestingly, knockout *OsCDKF;2* by CRISPR-Cas9 greatly reduced of parenchyma cell number in spikelets, with reductions of up to 22.28% and 12.02% in *cdkf;2* and *ARF12 OE-cdkf;2* mutants compared to WT and *ARF12 OE*, respectively (Figure 6H and Figure 6I). These results indicated that *OsCDKF;2* positively regulates grain filling by increasing cell division to enhance grain size and weight in rice.

Gene regulatory network analysis of *miR167-OsARF12* module

To elucidate the downstream gene regulatory network of *miR167-OsARF12* module in rice grain development, high throughput RNA-sequencing analysis of developing grains from *ARF12 OE*

plants was done. In total, we got 7174 differentially expressed genes (DEGs) with at least a 2-fold change between WT and *ARF12 OE* plants. Of the DEGs, 6,229 were upregulated and 945 were downregulated, which corroborates the role of OsARF12 as a transcription factor (Supplemental Figure 10B). Additionally, we found 1123 transcription factor genes and 913 protein kinase genes in the DEGs (Supplemental Figure 11). Biological processes related to cell development, hormone signaling, seed size regulation, sucrose and starch metabolism showed significant enrichment among the DEGs (Supplemental Figure 10A and Supplemental Figure 10C and Supplemental Figure 10D and Supplemental Figure 10E and Supplemental Figure 10F). Interestingly, we also observed enrichments in pathways associated with IAA and BR metabolism and signaling (Supplemental Figure 10C).

Specifically, expressions of DEGs related to cell development including cyclins, CDKs, cell expansion and CELLULOSE SYNTHASE A (CESA) were analyzed. Our analysis showed that majority of cyclins and CDK members as well as CESAs were upregulated in *ARF12 OE* plants but downregulated in *ARF12 RNAi* plants compared to WT plants (Supplemental Figure 10C and Supplemental Figure 10F and Supplemental Figure 12). Furthermore, cell numbers in the lemma along the longitudinal axis were significant higher in *ARF12 OE* plants relative to wild type (Supplemental Figure 13). These results strongly suggested that the *miR167-OsARF12* module plays vital roles in regulating genes involved in cell cycle and cell proliferation determination during grain development. In addition, DEGs that participate in the synthesis of IAA and BR processes such as *OsASB1*, *OsYUCCA7*, *OsD11*, and *OsDWARF*, as well as signaling genes including *OsTIR1*, *OsARF12*, *OsBRI1* and *OsBZR1* were upregulated in *ARF12 OE* plants (Supplemental Figure 10C) but downregulated in *ARF12 RNAi* plants, as confirmed by qRT-PCR (Supplemental Figure 12). Collectively, these results underscored the positive influence of the *miR167-OsARF12* module plays a positive role in the regulation of cell development and IAA, BR signaling to enhance grain filling.

Sensitivity determination to exogenous auxin and BR of *ARF12 OE* plants and *ckdf;2* mutants

To investigate the possibility of *OsCDKF;2* targeted by *OsARF12* mediating auxin signaling, root elongation assay in WT, *ARF12 OE* plants and *cdkf;2* mutants was firstly performed under 2,4-D treatment. Three-day-old seedlings were transferred to a nutrient solution containing various concentrations of 2,4-D. At 50 nM 2,4-D treatment for 3 days, the root elongations of *ARF12 OE*

seedlings decreased significantly compared to that of WT (Supplemental Figure 14A). Moreover, the root elongation of *ARF12 OE* also exhibited a significantly stronger sensitivity to 200 nM 2,4-D than that of the WT, with their elongation rates being 34.07% (P<0.01), 53.65% (P<0.01) and 58.00% (P<0.01) in *ARF12 OE*-5, -13 and -15 plants, respectively, while the WT's elongation rate was 68.22% (Supplemental Figure 14B). Given that overexpression of *OsARF12* affected root elongation under 2,4-D treatment, we sought to determine whether *OsARF12* expression was itself auxin-responsive in the WT. Our data revealed that *OsARF12* expression was transiently activated during IAA treatment in the WT (Supplemental Figure 14C). In contrast, *cdkf;2* mutants showed reduced sensitivity to auxin signaling (Supplemental Figure 15 A and Supplemental Figure 15B). Together with the increased or decreased expression of the auxin receptor gene *OsTIR1* in *ARF12 OE* plants or in *cdkf;2* mutants (Supplemental Figure 10C and Supplemental Figure 16), we showed that *OsCDKF;2* targeted by *OsARF12* participated in the process of auxin signal transduction.

To understand the involvement of *OsCDKF;2* targeted by *OsARF12* in BR signaling, we conducted three classical BR sensitivity experiments including coleoptile elongation, root growth and degree of leaf inclination of wild type and *ARF12 OE* plants in presence of 24-epibrassinolide (24-eBL) (Supplemental Figure 14D). Our findings revealed that *ARF12 OE* plants exhibited a significant increase in coleoptile elongation as compared to the WT under 1 μM 24-eBL treatment. Specifically, the maximum elongation of *ARF12 OE* was approximately as three times as that of the WT (Supplemental Figure 14E). In contrast to coleoptile elongation, primary root (PR) growth was inhibited by BR treatment. The reduction of PR was 1.78-1.92 cm in *ARF12 OE* plants, while it was 1.06 cm in WT (Supplemental Figure 14F). Moreover, *ARF12 OE* plants also showed a significant increase in the angle of the lamina joint by 13.26-34.39% under 24-eBL treatment compared to the WT (Supplemental Figure 14G). These results implied that *OsARF12* positively regulates BR signaling in rice. Nevertheless, *cdkf;2* mutants responded slightly to 24-eBL treatment, demonstrating that *cdkf;2* knock out lines were less sensitive to exogenous BR treatment (Supplemental Figure 15C and Supplemental Figure 15D and Supplemental Figure 15E and Supplemental Figure 15F), suggesting that *OsCDKF;2* targeted by *OsARF12* might be involved in regulating multiple steps of the BR signaling pathway. This hypothesis was supported by observations of up-regulated or down-regulated expression levels of BR biosynthetic genes such as

401 *OsD11*, *OsDWARF* as well as BR signaling genes such as *OsBRI1* and *OsDLT1* in *ARF12 OE* plants
402 or in *cdkf;2* mutants (Supplemental Figure 10C and Supplemental Figure 16).

403 **DISCUSSION**

404 In this study, we propose that *miR167-OsARF12* module might act downstream of miR159, and may
405 promote cell division by mediating auxin and BR signals to regulate rice grain filling through
406 targeting *OsCDKF;2* (Figure 7). Firstly, we found that suppressed expression of miR167
407 significantly improved grain weight and yield by enhancing grain filling and revealed the possible
408 regulatory effects of miR159 on miR167. Secondly, we demonstrated that *OsARF12* was the main
409 target of miR167 in the regulation of grain development by controlling cell division. Moreover, we
410 showed that the TGTCGG element in the *OsCDKF;2* promoter directly interacts with OsARF12,
411 and the luciferase reporter assay confirmed that OsARF12 activates *OsCDKF;2*. The results of the
412 luciferase reporter assay indicated that OsARF12 could activate the expression of *OsCDKF;2*.
413 Consistent with this, *cdkf;2* knock out lines, created by CRISPR Cas9 technology, sharply reduced
414 grain size and weight through decreasing grain filling. Thirdly, DEGs analysis indicated enrichment
415 of genes involved in auxin, BR biosynthesis, signaling and cell development processes between WT
416 and *ARF12 OE* plants. Furthermore, *ARF12 OE* plants are sensitive to exogenous IAA and BR
417 treatment, whereas *cdkf;2* mutants reduced sensitivity to auxin and BR signaling, indicating that
418 *OsCDKF;2* targeted by *OsARF12* may mediate auxin and BR signaling.

419 *miR167* is a conserved miRNA known to target *ARFs* in various plant species (Luo et al., 2013).
420 Previous researches have established a relationship between altered rice *miR167* expression and
421 plant architecture, including plant height, tiller number, panicle length, and tiller angle, as well as
422 immunity against *M. oryzae* (Liu et al., 2012; Li et al., 2020; Zhao et al., 2019b). A recent study
423 highlighted the role of *miR167a-OsARF6-OsAUX3* module regulates grain length and weight in rice,
424 where the overexpression of *miR167a* led to a higher length/width ratio compared to WT (Qiao et
425 al., 2021). The *miR167* family consists of ten members (*miR167a-j*) and perhaps each member has
426 individual function(s) and its expression pattern may vary. For example, different groups within
427 *miR156* family regulate various agronomic traits of rice (Miao et al., 2019), suggesting that
428 individual members within *miR167* family may exhibit diverse functions. In this study, we
429 suppressed the expression of *miR167* by STTM or Mimic aiming to inhibit the expression of all

members of *miR167*. Here, suppressed expression of *miR167* by means of STTM or Mimic driven by the endosperm-specific promoter Gt13a significantly increased grain length and width, which is consistent with our previous research (Peng et al., 2018) (Figure 1). Furthermore, statistical analysis based on multi-point (Zhengzhou & Shanghai) experiments from 2015-2018 showed that grain length/width ratio of *STTM167* plants and *MIM167* plants did not significantly differ from that of the wild type (Supplemental Table 3).

OsARF12, a downstream target of *miR167*, mediates auxin synthesis or signaling and functions during different stages of plant development. It has been reported that *OsARF12* is a transcription activator, which is inhibited by *OsmiR167d* as shown by a transient expression assay in tobacco and rice callus. *OsARF12* is essential for root elongation by modifying the expressions of auxin synthesis genes, *OsYUCCAs* and auxin efflux carriers, *OsPINs* and *OsPGPs* (Qi et al., 2012b). Knocking out of *OsARF12* made the *osarf12* mutants lose sensitivity to NPA treatment and affected auxin accumulation under the Pi deprivation condition (Wang et al., 2014). *OsARF12* positively regulates rice immunity against *M. oryzae*, presumably via IAA-JA crosstalk (Zhao et al., 2019b). In the present study, one more potential role of *miR167-OsARF12* in seed development and grain weight determination through regulating grain filling was unfolded. Specifically, both maximum filling rate and average filling rate were improved in *STTM/MIM167* plants (Figure 1H and Figure 1I and Supplemental Table 1). And as the main target of *miR167* in grain filling, overexpression of *OsARF12* could mimic the phenotype of *STTM/MIM167* plants in aspects of grain filling and weight (Figure 4H and Figure 4I and Supplemental Table 4). Thus, these findings contribute to a more thorough understanding of the biological function of the *miR167-OsARF12* module, which might be a potential target for high-yield breeding of rice.

Cyclins, cyclin-dependent kinases (CDKs), and several other proteins control the progression of the plant cell cycle. CDKs are Ser-Thr protein kinases that are crucial in cell cycle regulation during the embryonic and postembryonic development in different organisms (Malumbres, 2014). CDKs play a pivotal role in a highly conserved molecular mechanism that controls the progression of the cell cycle (Dudits et al., 2015). One CDKF was identified in *Arabidopsis* (AtCDKF;1) and four rice CDKs (CDKF;1-4) share high degree of homology with AtCDKF;1 (Guo et al., 2007). Here we showed that, as the main target of *miR167* in determining grain filling, OsARF12 could bind directly

to the promoter region of *OsCDKF;2* and activate its expression. By amino acid sequence alignment, a conserved protein domain, S-TKc, was found both in AtCDKF;1 and OsCDKF;2 (Supplemental Figure 16). Therefore, we hypothesized that *OsCDKF;2* might share some similar function with *AtCDKF;1*.

It has been documented that knockout mutants of *CDKF;1* had severe defects in cell division, cell elongation and endoreduplication during post-embryonic development (Takatsuka et al., 2009). In this study, we firstly analyzed a co-expression network of *OsCDKF;2* and the expression patterns of its co-expressed genes during grain development (Supplemental Figure 18A). The analysis indicated a relatively high expression level of most co-expressed genes along with grain filling, implying the potential involvement of *OsCDKF;2* in grain development. Furthermore, pathways analysis of co-expressed genes revealed significant enrichment of cellular biosynthesis and regulation, response to hormones, and nutrient substance transport (Supplemental Figure 18B). And the expression of co-expressed genes in *ARF12 OE* and *ARF12 RNAi* plants was confirmed by qRT-PCR (Supplemental Figure 18C and Supplemental Figure 18D). Of interest, we discovered that expression of *OsCDKF;2* was significantly upregulated in 5 DAF grains of *ARF12 OE* transgenic plants. Besides *OsCDKF;2*, expressions of its co-expressed genes and other rice core cell cycle genes (*OsCycA1;1*, *OsCycA1;4*, *OsCycA2;1*, *OsCycB1;1*, *OsCycB2;2*, *OsCycD1;2, OsCKL1*, *OsCKL2*, *OsCKL10*), cell wall synthase genes (*OsCSLA1*, *OsCSLC1*), and cellulose synthase gene (*OsCESA1*) were upregulated or downregulated in 5 DAF grains of *ARF12 OE* transgenic plants or *cdkf;2* mutants (Supplemental Figure 10F and Supplemental Figure 16). Considering the promotion of cell division rate during spikelet development and increased cell number in the lemma along the longitudinal axis of spikelet hulls of *ARF12 OE* plants compared with wild type, as well as the decreased cell number in grain spikelet hulls before heading stage of *cdkf;2* mutants and *ARF12 OE-cdkf;2* mutants compared with their individual controls (Figure 4L and Figure 4M and Supplemental Figure 13 and Figure 6H and Figure 6I), it was reasonable to believe that the grain size and weight of *ARF12 OE* plants or *cdkf;2* mutants may be regulated, or at least partially, by the accelerated or reduced cell division rate in the spikelet hulls.

It is also well-established that the cell cycle is influenced by extracellular cues and plant hormones, such as ABA, cytokinin and auxin (La et al., 2006). Auxin has been extensively documented for its

role in controlling the transcription of the cell cycle genes (Guo et al., 2007). Consistent with previous studies that the expressions of many core cell cycle genes were regulated by auxin, the transcriptional level of *OsCDKF;2* was extensively induced under 10 μM IAA treatment (Supplemental Figure 18E), which was consistent with the idea we proved in the present study that *OsCDKF;2* targeted by *OsARF12* mediates auxin signaling (Supplemental Figure 14A and Supplemental Figure 14B and Supplemental Figure 14C). Studies have been reported that auxin regulates seed growth and development by promoting cell division or cell expansion in the spikelet hulls and that *BG1* may play a role in auxin transport and grain size control through regulation of cell proliferation and expansion (Liu et al., 2015). Additionally, *OsSK41* and *OsARF4* control grain size through auxin-mediated cell expansion in the spikelet hulls (Hu et al., 2018). Besides IAA, pathways involved in BR biosynthesis and signaling were also enriched in the DEGs between WT and *ARF12 OE* plants. Previous studies reported that BR also modifies cell development processes to control seed size and weight. OsPPKL proteins, which share some similarities with *Arabidopsis* BSU1, act in BR signal transduction to promote cell division and elongation (Zhang et al., 2012). What's more, OsPPKL1 can interact with and dephosphorylates Cyclin-T1;3, and reducing its expression downregulates grain size in rice (Qi et al., 2012a). Therefore, we propose that *OsCDKF;2* targeted by *OsARF12* might regulate grain filling and grain size by increasing cell division and enhancing both auxin and BR signaling.

Previous research reported that the application of exogenous auxin during the grain filling stage can lead to a significant increase in rice grain filling rate and 1,000-grain weight (Abu-Zaitoon et al., 2012). Recent evidence on pea indicates that auxin is a key factor in mediating the switch from sucrose to hexoses, and impairment of auxin biosynthesis in the *tar2-1* mutant has been shown to specifically affect the seed filling stage by curtailing embryo growth and sucrose partitioning into reserve starch (Mcadam et al., 2017; Meitzel et al., 2020). In addition, BR regulates grain filling in rice stimulating the flow of assimilation from the source to the ink (Wu et al., 2008). And BR synthesis and signal transduction-related genes such as *D11*, *OsBRI1*, and *BAK1* positively regulate rice grain size and rice grain filling rate (Khew et al., 2015; Tanabe et al., 2005; Tong et al., 2012). What's more, auxin also promotes the expression of genes related to BR biosynthesis (Chung et al., 2011). *OsARF17* and *OsARF19* have been shown to control rice leaf inclination by regulating both

auxin and BR signaling or their cross-talk (Chen et al., 2018; Zhang et al., 2015). Here, in the present study, we found that the expression of *OsARF12* and *OsCDKF;2* was induced by IAA treatment and *ARF12 OE* seedlings or *cdkf;2* mutants were more or less sensitive to exogenous auxin and 24-eBL treatment when compared with WT (Supplemental Figure 13 and Supplemental Figure 14). Furthermore, genes related to auxin and BR synthesis and signal transduction were significantly upregulated in *ARF12 OE* plants and downregulated in *ARF12 RNAi* plants (Supplemental Figure 10C and Supplemental Figure 11). These findings suggested that *OsCDKF;2* targeted by *OsARF12* plays a vital role in rice grain filling by mediating auxin and BR signaling, but the inner mechanisms remain to be further investigated.

Grain filling is the key stage of grain formation and characteristics such as grain filling rate, grain filling duration and network among various environmental factors determine final yield and quality. The present study analyzed the effects of genetic modifications on the maximum and mean filling rates in rice plants. The results showed that *STTM167/MIM167* and *ARF12 OE* plants exhibited significant increases in both parameters, while *ARF12 RNAi* plants experienced decreases compared to the wild type plants. Notably, starch is the main component of rice grain, making the sucrose-starch metabolism and transport critical for grain filling. Grain filling-related genes include sucrose synthesis genes *OsSuS1-6*, starch synthesis genes- *OsSSI*, *OsSSIIa*, *OsSSIIb*, *OsGBSSI*, *OsGBSSII* and *OsAGPL1/2* (ADP-glucose pyrophosphorylase, AGPase). *OsCIN1*, which is responsible for sucrose unloading in endosperm during early grain filling, *OsAGPL1* (rate-limiting enzymes in starch synthesis), *OsGFR1* (Grain filling rate), *OsSUT4* (Sucrose transporter), *OsSUT5*, *OsMADS29*, *OsDOF11* and so on, are positive regulators controlling rice grain filling. Any and mutation in them would lead to reduced filling rate or abnormal grain filling (Naohiro et al., 2003; Ohdan et al., 2005; Yin and Xue, 2012).

And some seed size Quantitative Trait Loci (QTLs), such as *GW8*, *GS5*, *GS2*, and *GLW7* have also been reported to positively contribute to grain filling by promoting cell development process like cell division, cell expansion, or cell elongation (Li et al., 2019). Besides, *OsRac1*, belonging to the Rho-family GTPase, regulates rice grain filling and size via cell division (Zhang et al., 2019), while *OsUBP15*, which encodes a deubiquitinase protein, enhances protein stability, and contributes to rice grain filling (Shi et al., 2019). In addition, a very recent study confirms that trehalose 6-

phosphate promotes seed filling by activating auxin biosynthesis, and *OsTPP7* is responsible for T6P synthesis in rice (Meitzel et al., 2020). Here, expressions of all the mentioned above genes were upregulated in *ARF12 OE* plants according to our RNA-seq data (Supplemental Figure 10D and Supplemental Figure 10E), whereas *cdkf;2* mutants show an opposite trend (Supplemental Figure 16). Therefore, the altered grain filling rate of *OsARF12* transgenic plants and *cdkf;2* mutants is partially due to the changed expressions of grain filling-related genes.

MATERIALS AND METHODS

Plant materials

Rice (*Oryza sativa* L.) Japonica cultivar *Nipponbare* (NIP) was used in this study. Transgenic plants including suppressed expression of *miR167* plants (*STTM167* and *MIM167*), overexpression of *OsARF12* plants (*ARF12 OE)* and RNAi interference plants (*ARF12 RNAi*) were produced in our lab. Homozygous lines of each transgenic plant were used in this study. Rice plants used in this study were grown under non-stressed conditions at a research farm of Henan Agricultural University (Zhengzhou, Henan Province) under natural conditions.

Plasmids construction and plant transformation

The Short Tandem Target Mimic (STTM) and target mimic (MIM) were used to construct the vectors suppressing the expression of *miR167*. The STTM fragment with restriction sites *KpnI* and *BamHI* (5'-GGTACC(KpnI)TAGATCATGCTCTA(insertion)GGCAGCTTCAGTTGTTGTTGTTATGGTCTAATTTAAATATGGTCTAAAGAAGAAGAAT(Spacer)CAGATCATGCTCTA(insertion)GGCAGCTTCAGGATCC (*BamHI*) -3') and the sequence of target mimic of *miR167* with the same restriction sites (5'-GGTACC (*KpnI*) TCTACTAAGGCAGATCATGCTCAA(insertion)GGCAGCTTCAATTATTCGGTGGATCC (*BamHI*) -3') (the italics are the skeleton structure of *INDUCED BY PHOSPHATE STARVATION1* (*IPS1*); the underlined sequences represent binding sites of *miR167*) were synthesized by Sangon Biotech (Shanghai, China) and inserted downstream of the Gt13a promoter in pCAMBIA1301. To make transgenic lines overexpressing *OsARF12,* gene-specific primers were used to amplify the whole CDS sequence including 2457 bp form mRNA of NIP according to a reference sequence in

Rice Functional Genomic Express Database (http://signal.salk.edu/cgi-bin/RiceGE). And the product of PCR was inserted in a basal vector fused with Flag protein owned by our lab under the promoter of Ubi. To make the RNAi interference vector, about 60 bp specific sequence in the coding region of *OsARF12* was selected as the interference fragment. Two long oligonucleotides with complementary sequences containing 9-nt at 3' end were synthesized according to the sequence of target fragments. Then the synthesized fragments were cloned into the pCAMBIA1301 under the promoter of Gt13a with restriction sites *BamHI* and *KpnI*. For the *OsARF12-eGFP* construct, the full-length *OsARF12* cDNA was amplified by PCR and inserted into pGreen-eGFP using seamless Cloning (ClonExpress II One Step Cloning Kit, C112-02, Vazyme, China). *OsCDKF;2* mutant lines were constructed using CRISPR/Cas9 with the expression vector pEGCas9Pubi-N. The sequence of the target site was 5'-CCGGACGACAGGGGAGACCGTCG-3', which contained a protospacer adjacent motif (PAM) CCG at the 5' end. All constructs were introduced into *Agrobacterium tumefaciens* strain EHA105 cells for the subsequent transformation of *Nipponbare* rice plants as described previously. Details regarding the primers used for constructing vectors are provided in supporting information in Supplemental Table 5.

Grain trait and filling parameters determination

The homozygous T3 generation plants were used for a panicle and grain phenotypic analysis. The grain length, width, and thickness were measured by an electronic digital display vernier caliper and filled grains were used for measuring the 1,000-grain weight. The plant height, primary and secondary branch number, panicle length, and grain number per panicle were obtained from the measurement of the main stem. Filling parameters of wild-type and transgenic plants were fitted according to Richards' equation and detailed methods were referred to previous research (Zhao et al., 2019a).

Subcellular localization

To generate the *35S::OsARF12-eGFP* plasmid, the full-length *OsARF12* coding sequence without the stop codon was inserted into the pGreen-eGFP vector between the *BamHI* and *SmaI* sites. Rice protoplasts were transformed with the *35S::OsARF12-eGFP* construct as described previously. GFP signals were observed with the LSM710 confocal microscope (Zeiss, German).

qRT-PCR analysis

Total RNAs were isolated from various plant organs or grains using Trizol reagent (Invitrogen) or TransZol Plant (Transgen, ET121-01) according to the manufacturer's instructions. First-strand cDNAs were synthesized from 1 μg total RNA using a Quantscript RT Kit (Tiangen, KR103). Stem-loop qPCR was used for detecting the expression of *miR167*. For qRT-PCR, Taq Pro Universal SYBR qPCR Master Mix (Vazyme, Q712-02) was added to the reaction system and run on the BioRad iQ5 sequence detection system (BioRad, Hercules, CA) and the β-actin gene was used as an internal control. The relative expression level was calculated by $2^{-\Delta\Delta Ct}$. The primers used were listed in Supplemental Table 5. The PCR procedure was: 95 °C for 30 s, followed by 40 cycles of 95 °C for 5 s, 60 °C for 15 s and extension at 72 °C for 30 s.

Scoring matrix analysis

All 2 kb upstream sequences of genes as promoter region extracted from the RAP rice genome (released by the Rice Annotation Project Database and Resource). The transcription factor (TF) binding profiles of OsARF12 was downloaded from JASPAR and PlantTFDB (Plant Transcription Factor Database) (Fornes et al., 2019). We searched all exact matches in 2 kb promoter regions using the position-specific scoring matrices (PSSM) score computed from the OsARF12 binding profile and setting the threshold of false-negative rate (FNR) below 0.001. Please refer to biopython instructions (http://biopython.org/) for the detail method of searching matches.

Yeast-one-hybrid assays

Y1H assays were used to determine binding of OsGAMYBL2 and OsARF12 to the *miR167* and *OsCDKF;2* promoters, respectively. The predicted binding sites of the *miR167h* and *OsCDKF;2* promoter with three tandem repeats were synthesized and inserted into the pHis2 vector between *EcoRI* and *SacI*. The full-length of *OsGAMYBL2* and *OsARF12* CDS were amplified and inserted into the pGADT7-Rec2 vector between *EcoRI* and *SmaI*. Yeast cells were grown on selective dropout media with SD/-Trp-Leu/-His (TDO) including different concentrations of 3-amino-1,2,4-triazole (3-AT).

ChIP-qPCR

Briefly, young panicles of flowering and 5 DAF grains of *Ubi::OsARF12-3*FLAG* rice plants and seedlings of *Ubi::OsGAMYBL2-3*FLAG* were cross-linked in 1% formaldehyde then a ChIP assay was performed according to the previous research (He et al., 2005). Immunoprecipitations were performed using an anti-FLAG polyclonal antibody (Cell Signaling Technology, #14793, U.S.), with normal IgG used as a negative control. The purified precipitated DNA was dissolved in TEN buffer (Tris-EDTA-NaCl) for a qRT-PCR analysis. The primers used in the ChIP-qPCR assays are listed in Supplemental Table 5.

Relative luciferase activity measurement *in vivo*

The transcriptional activity assay was carried out in the transient-transformed protoplast prepared from 10-day-old rice etiolated seedlings of the wild type line grown in darkness conditions as described previously (Lin et al., 2007). For the specific binding and activating activity of OsGAMYBL2 and OsARF12 to the *miR167h* and *OsCDKF;2* promoter assay, full-length cDNA of *OsGAMYBL2* and *OsARF12* were fused into the pGreen-eGFP vector driven by the CaMV 35S promoter to generate *pGreen-OsGAMYBL2-GFP* and *pGreen-OsARF12-GFP*. The pGreen-GFP vector was used as the negative control. The promoter of *miR167h* (-2370 bp) and *OsCDKF;2* (-1874 bp) were amplified and inserted into pGreenII-008 with LUC and REN to generate the *miR167h::LUC* and *OsCDKF;2::LUC* reporter gene, respectively. REN gene was driven by the 35S promoter and the fluorescent reading (LUCRenilla) was used as an internal reference. LUC gene was driven by the inserted promoter of *miR167h* and *OsCDKF;2* and fluorescent reading recorded as LUC Firefly. And the transcriptional activity of OsGAMYBL2 in *Nicotiana benthamiana* leaves was examined as described previously (Song et al., 2017). The cDNA of *OsGAMYBL2* was cloned into pCAMBIA1300 carrier to form the effector plasmid. The reporter and effector constructs were inserted separately into *A. tumefaciens* strain GV3101 cells for the subsequent co-infiltration of *N. Benthamiana* leaves. The LUC signals were detected with the automatic chemiluminescence image analysis system (Tamon 5200, Shanghai, China). Ratio of LUC Firefly / LUC Renilla measured on GloMax20/20 (Promega, U.S.) represented the transcription regulation effect of OsGAMYBL2 and OsARF12 on *miR167h* and *OsCDKF;2*, respectively. Dual Luciferase Reporter Gene Assay Kit (11402ES60, Yeasen, China) was used to measure relative luciferase activity.

Histological analysis

For histological analysis, spikelet hulls before flowing of wild type, *ARF12 OE*, *cdkf;2 mutants* and *ARF12 OE-cdkf;2* mutants were placed in Formalin-acetic acid-alcohol (FAA) solution. Then samples were dehydrated in a graded ethanol series followed by embedding. The samples were dissected and then observed under a light microscope (80I; Nikon, Kanagawa, Japan). The outer surfaces of the lemmas of wild type and *ARF12 OE* plants were observed with the Sigma 500 scanning electron microscope (Zeiss, UK) at an acceleration voltage of 5.0 kV.

Nucleus isolation and assessment of ploidy

The young panicles of WT and *ARF12 OE* plants with the same length were chopped with a sharp blade soaking in the cool Galbraith's buffer: 45 mM MgCl2, 20 mM MOPS, 30 mm Sodium citrate, 0.1%[v/v] Triton X-100 (PH=7.0). After filtering through a 40 μm nylon riddle, the nucleus suspension was added propidium iodide (PI) for a few minutes and then was loaded into the flow cytometer (BD FACSCelesta, America). For each detection, the ploidy of 10000 nuclei were recorded and the results were analyzed with Flowjo 10 software

RNA-seq analysis

Spikelets of wild type (WT) and *ARF12 OE* plants at 5 DAF transgenic plants were collected for total RNA extraction. The isolated RNAs sequencing was done with the service from BGI (Shenzhen, China). Differentially expressed genes (DEGs) between WT and ARF12 OE transgenic plants. The DEGs with fold changes > 1.5 and FDR (false discovery rates) < 0.05 were defined as differentially expressed and used for further GO enrichment analysis. BiNGO was used to analyze item classification of differentially expressed genes (Maere et al., 2005). *P*-value of each GO item classification was calculated by hypergeometric test and was further checked by means of Benjamin & Hochberg. GO item classification involved at least five genes and checked *P*-value, < 0.05, was considered enriched, significantly.

IAA and BR treatment

To detect IAA sensitivity, 3-day-old seedlings of *Nipponbare* (WT), *ARF12 OE*, *cdkf;2* and *ARF12 OE-cdkf;2* mutants were transferred to a nutrient solution containing 50 nM and 200 nM 2,4-D for four days. And PR length was measured to evaluate the response effect of auxin on OsARF12. For auxin instantaneous response, expression of *OsARF12* in one-week-old *Nipponbare* (WT) seedlings

686 was detected under 10 μM IAA or 1μM 2,4-D treatment for 3h.

687 For BR treatment, rice seeds were sterilized with 10% $NaClO_3$ and grown in 1/2 Murashige and
688 Skoog (MS) medium (M519, Phytotech, China) with 1 μM 24-eBL for one week under dark
689 condition. Then coleoptile lengths were photographed and measured. For PR inhibition analysis,
690 germinated seeds were grown in normal culture solution supplemented with 1 μM 24-eBL for 7 d
691 and PR length was measured. Leaf angles between the second leaf blade and sheath were measured
692 after 8 d in a dark growth and 3 d incubation with 1 μM 24-eBL.

693 **Data availability**

694 Raw reads generated in this study were deposited in the NCBI (https://www.ncbi.nlm.nih.gov) SRA
695 database as bioproject PRJNA956125 and the National Genomics Data Center
696 (https://ngdc.cncb.ac.cn) as GSA of CRA016640.

697 **FUNDING**

698 This work was funded by National Natural Science Foundation of China (NSFC 32272014,
699 32001440, 31971846 and 31871554), Natural Science Foundation of Henan Province-Excellent
700 Youth Fund (222300420049), Central Plains Talents Program of Henan Province (Talent Training
701 Series) - Top Young Talents in Central Plains (ZYYCYU202012170), Support Plan for Scientific
702 and Technological Innovation Talents in Colleges and Universities of Henan Province
703 (21HASTIT037) and China Postdoctoral Science Foundation (2020M682294).

704 **AUTHOR CONTRIBUTION**

705 T.P., Q.Z., and H.X. conceived and designed the project; Y.Z., X.Z., Y.C., and X.D. conducted the
706 experiments; Y.Z., S.T., C.M., H.S., analyzed the data; Y.Z., H.X., X.Z., and Y.C. wrote the
707 manuscript; T.P., Q.Z., G. T., and G. F. revised the manuscript.

708 **ACKNOWLEDGMENTS**

709 No conflict of interest is declared.

710 **REFERENCES**

711 **Abu-Zaitoon, Y.M., Bennett, K., Normanly, J. and Nonhebel, H.M.** (2012). A large increase in

712 IAA during the development of rice grains correlates with the expression of tryptophan
713 aminotransferase OsTAR1 and a grain-specific YUCCA. *Physiolo. Plantarum* **146**: 487-499.
714 **Bartel, D.P.** (2009). MicroRNAs: target recognition and regulatory functions. *Cell* **136**: 215-233.
715 **Chen, S.H., Zhou, L.J., Xu, P. and Xue, H.W.** (2018). SPOC domain-containing protein Leaf
716 inclination3 interacts with LIP1 to regulate rice leaf inclination through auxin signaling. *PLoS*
717 *Genet.* **14**; e1007829.
718 **Chung, Y., Maharjan, P.M., Lee, O., Fujioka, S., Jang, S., Kim, B., Takatsuto, S., Tsujimoto,**
719 **M., Kim, H. and Cho, S.** (2011). Auxin stimulates DWARF4 expression and brassinosteroid
720 biosynthesis in Arabidopsis. *Plant J.* **66**; 564-578.
721 **Duan, P., Ni, S., Wang, J., Zhang, B., Xu, R., Wang, Y., Chen, H., Zhu, X. and Li, Y.** (2015).
722 Regulation of OsGRF4 by OsmiR396 controls grain size and yield in rice. *Nat. Plants* **2**; 15203.
723 **Dudits, D., Cserháti, M., Miskolczi, P. and Horváth, G.** (2015). The Growing Family of Plant
724 cyclin-dependent kinases with multiple functions in cellular and developmental regulation.
725 *Annu. Plant Rev.* **32**; 1-30.
726 **Fornes, O., Castro-Mondragon, J.A., Khan, A., Lee, R. and Mathelier, A.** (2019). JASPAR 2020:
727 update of the open-access database of transcription factor binding profiles. *Nucleic Acids Res.*
728 **48**; D87–D92.
729 **Guo, C., Xu, Y., Shi, M., Lai, Y., Wu, X., Wang, H., Zhu, Z., Poethig, R.S. and Wu, G.** (2017),
730 Repression of miR156 by miR159 Regulates the Timing of the Juvenile-to-Adult Transition in
731 Arabidopsis. *The Plant Cell* **29**; 1293-1304.
732 **Gao, J., Chen, H., Yang, H., He, Y., Tian, Z. and Li, J.** (2018). A brassinosteroid responsive
733 miRNA-target module regulates gibberellin biosynthesis and plant development. *New Phytol.*
734 **220**; 636-650.
735 **Guo, J., Song, J., Wang, F. and Zhang, X.S.** (2007). Genome-wide identification and expression
736 analysis of rice cell cycle genes. *Plant Mol. Biol.* **64**; 349-360.
737 **He, J.X., Gendron, J.M., Sun, Y., Gampala, S., Gendron, N., Sun, C.Q. and Wang, Z.Y.** (2005).
738 BZR1 Is a Transcriptional Repressor with Dual Roles in Brassinosteroid Homeostasis and
739 Growth Responses. *Science* **307**; 1634-1638.
740 **Hu, J., Wang, Y., Fang, Y., Zeng, L., Xu, J., Yu, H., Shi, Z., Pan, J., Zhang, D., Kang, S., Zhu,**
741 **L., Dong, G., Guo, L., Zeng, D., Zhang, G., Xie, L., Xiong, G., Li, J. and Qian, Q.** (2015).

A rare allele of GS2 enhances grain size and grain yield in rice. *Mol. Plant* **8**; 1455-1465.

Hu, Z., Lu, S.-J., Wang, M.-J., He, H., Sun, L., Wang, H., Liu, X.-H., Jiang, L., Sun, J.-L., Xin, X., Kong, W., Chu, C., Xue, H.-W., Yang, J., Luo, X. and Liu, J.-X. (2018a). A Novel QTL qTGW3 encodes the GSK3/SHAGGY-Like kinase OsGSK5/OsSK41 that interacts with OsARF4 to negatively regulate grain size and weight in rice. *Mol. Plant* **11**; 736-749.

Khew, C.Y., Teo, C.J., Chan, W.S., Wong, H.L., Namasivayam, P. and Ho, C.L. (2015). Brassinosteroid insensitive 1-associated kinase 1 (OsI-BAK1) is associated with grain filling and leaf development in rice. *J. Plant Physiol.* **182**; 23-32.

La, H., Li, J., Ji, Z., Cheng, Y., Li, X., Jiang, S., Venkatesh, P.N. and Ramachandran, S. (2006). Genome-wide analysis of cyclin family in rice (*Oryza Sativa* L.). *Mol. Genet. Genomics* **275**; 374-386.

Li, N., Xu, R. and Li, Y.H. (2019). Molecular networks of seed size control in plants. *Annu Rev Plant Biol* **70**; 435-463.

Li, Y., Li, J.L., Chen, Z.H., Wei, Y., Qi, Y.H. and Wu, C.Y. (2020). OsmiR167a-targeted auxin response factors modulate tiller angle via fine-tuning auxin distribution in rice. *Plant Biotechnol. J.* **18**; 2015-2026.

Liu, H., Jia, S.H., Shen, D.F., Liu, J., Li, J., Zhao, H.P., Han, S.C. and Wang, Y.D. (2012). Four AUXIN RESPONSE FACTOR genes downregulated by microRNA167 are associated with growth and development in *Oryza sativa*. *Funct. Plant Biol.* **39**; 736-744.

Liu, L., Tong, H., Xiao, Y., Che, R., Xu, F., Hu, B., Liang, C., Chu, J., Li, J. and Chu, C. (2015). Activation of Big Grain1 significantly improves grain size by regulating auxin transport in rice. *Proc. Natl. Acad. Sci. USA* **112**; 11102-11107.

Luo, Y., Guo, Z. and Li, L. (2013). Evolutionary conservation of microRNA regulatory programs in plant flower development. *Dev. Biol.***380**; 133-144.

Maere, S., Heymans, K. and Kuiper, M. (2005). BiNGO: a Cytoscape plugin to assess overrepresentation of gene ontology categories in biological networks. *Bioinformatics* **21**; 3448-3449.

Malumbres (2014). Cyclin-dependent kinases. *Genome Biol.* **15**; 122.

Mcadam, E.L., Meitzel, T., Quittenden, L.J., Davidson, S.E., Dalmais, M., Bendahmane, A.I., Thompson, R., Smith, J.J., Nichols, D.S. and Urquhart, S. (2017). Evidence that auxin is

required for normal seed size and starch synthesis in pea. *New Phytol.* **216**; 193-204.

Mcdonald, B. (2012). Food Security Emerges as a Complex Global Challenge. *J. Conventional Weapons Destruction* **16**; 13.

Meitzel, T., Radchuk, R., McAdam, E.L., Thormählen, I., Feil, R., Munz, E., Hilo, A., Geigenberger, P., Ross, J.J., Lunn, J.E. and Borisjuk, L. (2020). Trehalose 6-phosphate promotes seed filling by activating auxin biosynthesis. *New Phytol.* **229**; 1553-1565.

Miao, C., Wang, Z., Zhang, L., Yao, J., Hua, K., Liu, X., Shi, H. and Zhu, J.K. (2019). The grain yield modulator miR156 regulates seed dormancy through the gibberellin pathway in rice. *Nature communications* **10**; 3822.

Naohiro, A., Tatsuro, H., Scofield, G.N., Whitfeld, P.R. and Furbank, R.T. (2003). The sucrose transporter gene family in rice. *Plant Cell Physiol.* **44**; 223-232.

Ohdan, T., Francisco Jr, P.B., Sawada, T., Hirose, T., Terao, T., Satoh, H. and Nakamura, Y. (2005). Expression profiling of genes involved in starch synthesis in sink and source organs of rice. *J. Exp. Bot.* **56**; 3229-3244.

Peng, T., Lv, Q., Zhang, J., Li, J.Z., Du, Y.X. and Zhao, Q.Z. (2011). Differential expression of the microRNAs in superior and inferior spikelets in rice (*Oryza sativa*). *J. Exp. Bot.* **62**; 4943-4954.

Peng, T., Qiao, M., Liu, H., Teotia, S., Zhang, Z., Zhao, Y., Wang, B., Zhao, D., Shi, L., Zhang, C., Le, B., Rogers, K., Gunasekara, C., Duan, H., Gu, Y., Tian, L., Nie, J., Qi, J., Meng, F., Huang, L., Chen, Q., Wang, Z., Tang, J., Tang, X., Lan, T., Chen, X., Wei, H., Zhao, Q. and Tang, G. (2018). A resource for inactivation of micrornas using short tandem target mimic technology in model and crop plants. *Mol. Plant* **11**; 1400-1417.

Peng, T., Sun, H.Z., Qiao, M.M., Zhao, Y.F., Du, Y.X., Zhang, J., Li, J.Z., Tang, G.L. and Zhao, Q.Z. (2014). Differentially expressed microRNA cohorts in seed development may contribute to poor grain filling of inferior spikelets in rice. *BMC Plant Biol.* **14**; 196.

Peng, T., Teotia, S., Tang, G. and Zhao, Q. (2019), MicroRNAs meet with quantitative trait loci: small powerful players in regulating quantitative yield traits in rice. *WIREs RNA* **10**; e1556.

Qi, P., Lin, Y.S., Song, X.J., Shen, J.B., Huang, W., Shan, J.X., Zhu, M.Z., Jiang, L., Gao, J.P. and Lin, H.X. (2012a). The novel quantitative trait locus GL3.1 controls rice grain size and yield by regulating Cyclin-T1;3. *Cell Res.* **22**; 1666-1680.

Qi, Y.H., Wang, S.K., Shen, C.J., Zhang, S.N., Chen, Y., Xu, Y.X., Liu, Y., Wu, Y.R. and Jiang, D.A. (2012b). OsARF12, a transcription activator on auxin response gene, regulates root elongation and affects iron accumulation in rice (*Oryza sativa*). *New Phytol.* **193**; 109-120.

Qiao, J., Jiang, H., Lin, Y., Shang, L., Wang, M., Li, D., Fu, X., Geisler, M., Qi, Y., Gao, Z. and Qian, Q. (2021). A novel miR167a-OsARF6-OsAUX3 module regulates grain length and weight in rice. *Mol. Plant* **14**; 1-14.

Rhoades, M.W., Reinhart, B.J., Lim, L.P., Burge, C.B., Bartel, B. and Bartel, D.P. (2002). Prediction of plant microRNA targets. *Cell.* **110**; 513-520.

Rosegrant, M.W. and Cline, S.A. (2003). Global food security: Challenges and policies. *Science* **302**; 1917-1919.

Shi, C., Ren, Y., Liu, L., Wang, F., Zhang, H., Tian, P., Pan, T., Wang, Y., Jing, R., Liu, T., Wu, F., Lin, Q., Lei, C., Zhang, X., Zhu, S., Guo, X., Wang, J., Zhao, Z., Wang, J., Zhai, H., Cheng, Z. and Wan, J. (2019). Ubiquitin Specific Protease 15 has an Important role in regulating grain width and size in rice. *Plant Physiol.* **180**; 381-391.

Takatsuka, H., Ohno, R. and Umeda, M. (2009). The Arabidopsis cyclin-dependent kinase-activating kinase CDKF;1 is a major regulator of cell proliferation and cell expansion but is dispensable for CDKA activation. *The Plant J.* **59**; 475-487.

Tanabe, S., Ashikari, M., Fujioka, S., Takatsuto, S., Yoshida, S., Yano, M., Yoshimura, A., Kitano, H., Matsuoka, M., Fujisawa, Y., Kato, H. and Iwasaki, Y. (2005). A Novel cytochrome P450 is implicated in brassinosteroid biosynthesis via the characterization of a rice dwarf mutant, dwarf11, with reduced seed length. *The Plant Cell* **17**; 776-790.

Tong, H., Liu, L., Jin, Y., Du, L., Yin, Y., Qian, Q., Zhu, L. and Chu, C. (2012). DWARF and LOW-TILLERING acts as a direct downstream target of a GSK3/SHAGGY-like kinase to mediate brassinosteroid responses in rice. *The Plant Cell* **24**; 2562-2577.

Wang, D.K., Pei, K.M., Fu, Y.P., Sun, Z.X., Li, S.J., Liu, H.Q., Tang, K., Han, B. and Tao, Y.Z. (2007). Genome-wide analysis of the auxin response factors (ARF) gene family in rice (*Oryza sativa*). *Gene.* **394**; 13-24.

Wang, J.-W. (2014). Regulation of flowering time by the miR156-mediated age pathway. *J. Exp. Bot.* **65**; 4723-4730.

Wang, S., Zhang, S., Sun, C., Xu, Y., Chen, Y., Yu, C., Qian, Q., Jiang, D.A. and Qi, Y. (2014).

Auxin response factor (OsARF12), a novel regulator for phosphate homeostasis in rice (*Oryza sativa*). *New Phytol.* **201**; 91-103.

Weijers, D. and Friml, J. (2009). SnapShot: Auxin Signaling and Transport. *Cell* **136**; 1172-1172e1171.

Wu, C.Y., Trieu, A., Radhakrishnan, P., Kwok, S.F., Harris, S., Zhang, K., Wang, J., Wan, J., Zhai, H., Takatsuto, S., Matsumoto, S., Fujioka, S., Feldmann, K.A. and Pennell, R.I. (2008). Brassinosteroids regulate grain filling in rice. *Plant Cell* **20**; 2130-2145.

Wu, Y.Z., Fu, Y.C., Zhao, S.S., Gu, P., Zhu, Z.F., Sun, C.Q. and Tan, L.B. (2016). CLUSTERED PRIMARY BRANCH 1, a new allele of DWARF11, controls panicle architecture and seed size in rice. *Plant Biotechnol. J.* **14**; 377-386.

Xia, K., Ou, X., Tang, H., Wang, R., Wu, P., Jia, Y., Wei, X., Xu, X., Kang, S.H., Kim, S.K. and Zhang, M. (2015). Rice microRNA osa-miR1848 targets the obtusifoliol 14alpha-demethylase gene OsCYP51G3 and mediates the biosynthesis of phytosterols and brassinosteroids during development and in response to stress. *New phytol.* **208**; 790-802.

Yang, J.H., Han, S.J., Yoon, E.K. and Lee, W.S. (2006). 'Evidence of an auxin signal pathway, microRNA167-ARF8-GH3, and its response to exogenous auxin in cultured rice cells'. *Nucleic Acids Res.* **34**; 1892-1899.

Yang, X., Zhao, X., Dai, Z., Ma, F., Miao, X. and Shi, Z. (2021). OsmiR396/Growth Regulating Factor modulate rice grain size through direct regulation of embryo-specific miR408. *Plant Physiol.* **186**; 519-533.

Yao, X.Z., Chen, J.L., Zhou, J., Yu, H.C.Z., Ge, C.N., Zhang, M., Gao, X.H., Dai, X.H., Yang, Z.N. and Zhao, Y.D. (2019). An essential role for miRNA167 in maternal control of embryonic and seed development. *Plant Physiol.* **180**; 453-464.

Yin, L.L. and Xue, H.W. (2012). The MADS29 transcription factor regulates the degradation of the nucellus and the nucellar projection during rice seed development. *Plant Cell* **24**; 1049-1065.

Zhang, S., Wang, S., Xu, Y., Yu, C., Shen, C., Qian, Q., Geisler, M., Jiang de, A. and Qi, Y. (2015). The auxin response factor, OsARF19, controls rice leaf angles through positively regulating OsGH3-5 and OsBRI1. *Plant Cell & Environ.* **38**; 638-654.

Zhang, X., Wang, J., Huang, J., Lan, H., Wang, C., Yin, C., Wu, Y., Tang, H., Qian, Q., Li, J.

and Zhang, H. (2012). Rare allele of OsPPKL1 associated with grain length causes extra-large grain and a significant yield increase in rice. *Proc. Natl. Acad. Sci. USA*. **109**; 21534-21539.

Zhang, Y., Xiong, Y., Liu, R., Xue, H.W. and Yang, Z. (2019). The Rho-family GTPase OsRac1 controls rice grain size and yield by regulating cell division. *Proc Natl Acad Sci USA*. **116**; 16121-16126.

Zhang, Y.C., Yu, Y., Wang, C.Y., Li, Z.Y., Liu, Q., Xu, J., Liao, J.Y., Wang, X.J., Qu, L.H., Chen, F., Xin, P., Yan, C., Chu, J., Li, H.Q. and Chen, Y.Q. (2013). Overexpression of microRNA OsmiR397 improves rice yield by increasing grain size and promoting panicle branching. *Nat. Biotechnol.* **31**; 848-852.

Zhao, D.S., Li, Q.F., Zhang, C.Q., Zhang, C., Yang, Q.Q., Pan, L.X., Ren, X.Y., Lu, J., Gu, M.H. and Liu, Q.Q. (2018). GS9 acts as a transcriptional activator to regulate rice grain shape and appearance quality. *Nat. Commun.* **9**; 1240.

Zhao, Y.F., Peng, T., Sun, H.Z., Teotia, S., Wen, H.L., Du, Y.X., Zhang, J., Li, J.Z., Tang, G.L., Xue, H.W. and Zhao, Q.Z. (2019a). miR1432-OsACOT (Acyl-CoA thioesterase) module determines grain yield via enhancing grain filling rate in rice. *Plant Biotechnol. J.* **17**; 712-723.

Zhao, Z.-X., Feng, Q., Cao, X.-L., Zhu, Y., Wang, H., Chandran, V., Fan, J., Zhao, J.-Q., Pu, M., Li, Y. and Wang, W.-M. (2019b). *Osa-miR167d* facilitates infection of *Magnaporthe oryzae* in rice. *J. Integr. Plant Biol.* **62**; 702-715.

Zhou, S.R., Yin, L.L. and Xue, H.W. (2013). Functional genomics based understanding of rice endosperm development. *Curr. Opin. Plant Biol.* **16**; 236-246.

Zhu, G.H., Ye, N.H., Yang, J.C., Peng, X.X. and Zhang, J.H. (2011). Regulation of expression of starch synthesis genes by ethylene and ABA in relation to the development of rice inferior and superior spikelets. *J. Exp. Bot.* **62**; 3907-3916.

885 **FIGURE LEGENDS**

886 **Figure 1. Suppressed expression of *miR167* enhances grain weight by accelerating grain filling**
887 **rate.** (A-B) Phenotypic observation of grain size of *Nipponbare* (WT), *STTM167* and *MIM167*
888 transgenic plants. Scale bars, 1 cm; (C) Validation of decreased expressions of rice *miR167* in
889 *STTM167* and *MIM167* transgenic plants, respectively, by stem-loop qRT-PCR; (D) Measurement
890 of the 1,000-hulled grain weight of *Nipponbare* (WT), *STTM167* and *MIM167* transgenic plants;
891 (E-F) Detailed analysis of grain traits including grain length (E), width (F) of *Nipponbare* (WT) and
892 *miR167* transgenic plants; (G) Yield per plot of *Nipponbare* (WT), *STTM167* and *MIM167*
893 transgenic plants in field test; (H) 1,000-hulled grain weight of *Nipponbare* (WT), *STTM167* and
894 *MIM167* transgenic plants at different stage of grain filling; (I) Fitted grain filling rate of *Nipponbare*
895 (WT), *STTM167* and *MIM167* transgenic plants at different stage of grain filling; (J) Morphologies
896 of seeds of *Nipponbare* (WT), *STTM167* and *MIM167* transgenic plants at different stage of grain
897 filling, Scale bar, 1mm. Experiments were repeated three times and data are presented as mean ±
898 SD (n=1000 grains); Statistical analysis was performed by Student's t-test (**, P<0.01; *, P<0.05).

899 **Figure 2. Morphological analysis of the cross between *STTM159* and *STTM167* as well as**
900 **biochemical analysis of the binding of OsGAMYBL2 on the *OsMIR167h* promoter.** (A)
901 Confirmation of transgenic plants of *STTM159*, crossed plants, *STTM167* and WT by 1% agarose
902 gel electrophoresis; (B) Grain morphology of the *Nipponbare* (WT), *STTM167*, *STTM159* and
903 crossed plants. Scale bars, 1 cm; (C) Measurement of the 1,000 grain weight of *Nipponbare* (WT),
904 *STTM159*, *STTM167* and cross plants, (n=3, n=1000 grains); (D) Grain length and width of the
905 *Nipponbare* (WT), *STTM167*, *STTM159*, and crossed plants, (n=3, n=1000 grains); (E-F)
906 Expression level of *miR167* in *STTM159* plants root (E) and shoot (F) by small RNA sequencing,
907 respectively; (G) Relative expression level of *miR167* in *Nipponbare* (WT), *STTM159* and
908 *STTM167* plants by qRT-PCR; (H) The Yeast one-hybrid assay of OsGAMYBL2 and the
909 *OsMIR167h* promoter in the presence of 50 mM 3-AT; (I-K) Luciferase reporter system analysis of
910 OsGAMYBL2 and the promoter of *MIR167h* by rice protoplast (I) and *N.benthamiana* (J-K); (L)
911 ChIP-qPCR analysis binding to the promoter of *miR167h2* region using FLAG antibody to enriched
912 DNA from seedlings of *OsGAMYBL2* transgenic plants. Experiments were repeated three times and
913 data are presented as mean ± SD; Statistical analysis was performed by Student's t-test (**, P<0.01;

914 *, $P<0.05$).

915 **Figure 3. *OsARF12* was validated as the main target of *miR167* in rice grain filling.** (A) Relative
916 expressions of *OsARF6*, *OsARF12*, *OsARF17*, *OsARF25* and *miR167* at 5 DAF (days after
917 fertilization), 10 DAF, 15 DAF, 21DAF, 27 DAF and 35 DAF by qRT-PCR and stem-loop qRT-PCR,
918 respectively. (B) Phenotypic observation of grain size of *Nipponbare* (WT), *ARF6 OE*, *ARF12 OE*,
919 *ARF17 OE* and *ARF25 OE* transgenic plants. Scale bar, 1 cm; (C) 1,000-grain weight of *Nipponbare*
920 (WT), O*RF6 OE*, *ARF12 OE*, *ARF17 OE* and *ARF25 OE* transgenic plants. (D) Correlation analysis
921 of expression level of *OsARF12* and grain weight in wild type and different *ARF12 OE* transgenic
922 lines; Experiments were repeated three times and data are shown as means ± SD; Statistical analysis
923 was performed by Student's *t*-test (**, $P<0.01$; *, $P<0.05$).

924 **Figure 4. *OsARF12* positively regulates grain filling and grain weight.** (A) Subcellular
925 localization analysis of OsARF12. Scale bar, 5 μm; (B-C) Phenotypic observation of grain size of
926 *Nipponbare* (WT) and *ARF12 OE* and *ARF12 RNAi* transgenic plants. Scale bars, 1 cm; (D)
927 Validation of decreased expressions of *OsARF12* in *ARF12 OE* and *ARF12 RNAi* transgenic plants,
928 respectively, by qRT-PCR; (E) Measurement of the 1,000 grain weight of *Nipponbare* (WT), *ARF12*
929 *OE* and *ARF12 RNAi* transgenic plants; (F-G) Detailed analysis of grain traits including grain length
930 (F), width (g) of *Nipponbare* (WT), *ARF12 OE* and *ARF12 RNAi* transgenic plants; (H) Yield per
931 plot of *Nipponbare* (WT), *ARF12 OE* and *ARF12 RNAi* transgenic plants in field test; (I) 1,000-
932 hulled grain weight of *Nipponbare* (WT), *ARF12 OE* and *ARF12 RNAi* transgenic plants at different
933 stage of grain filling; (J) Fitted grain filling rate of *Nipponbare* (WT), *ARF12 OE* and *ARF12 RNAi*
934 transgenic plants at different stage of grain filling; (K) Morphologies of seeds of *Nipponbare* (WT),
935 *ARF12 OE* and *ARF12 RNAi* transgenic plants at different stage of grain filling, Scale bar, 0.5 cm;
936 (L) The cell number counts that contain 2C DNA and 4C DNA in young panicles of WT and *ARF12*
937 *OE* transgenic plants; (M) Percentage comparison of the distribution of cells in different phases of
938 the cell cycle in young panicle cells of WT and *ARF12 OE* transgenic plants; Experiments were
939 repeated three times and data are presented as mean ± SD (n=1000 grains); Statistical analysis was
940 performed by Student's *t*-test (**, $P<0.01$; *, $P<0.05$).

941 **Figure 5. OsARF12 directly activates the expression of *OsCDKF;2*.** (A) Potential binding
942 sequence of OsARF12 calculated by scoring matrix analysis; (B) Increased or decreased expression

level of *OsCDKF;2* in *ARF12 OE* and *ARF12 RNAi* transgenic plants, respectively; (C) Localization of putative OsARF12 binding site in the *OsCDKF;2* promoter; (D) Yeast one-hybrid assay of OsARF12 and the promoter of *OsCDKF;2* in the presence of 80 mM 3-AT. Empty pGADT7-Rec2 vector was used as negative control; (E) Transactivation assay of OsARF12 with the luciferase reporter system; (F-G) ChIP-qPCR analysis of OsARF12 binding to the promoter of *OsCDKF;2* using FLAG antibody to enriched DNA from spikelet and panicle of *ARF12 OE* transgenic plants; Experiments were repeated three times and data are presented as mean ± SD; Statistical analysis was performed by Student's *t*-test (**, $P<0.01$; *, $P<0.05$).

Figure 6. Positive effects of *OsCDKF;2* on grain filling and grain size. (A) Comparisons of grains between *Nipponbare* (WT) and *cdkf;2* and *ARF12 OE-cdkf;2* mutants. Scale bars, 1cm; (B) Measurement of the 1,000-grain weight of *Nipponbare* (WT), *cdkf;2* and *ARF12 OE -cdkf;2* mutants. (n=3, n=1000 grains); (C-E) Grain length (C), width (D) and thickness (E) of the *Nipponbare* (WT), *cdkf;2* and *ARF12 OE -cdkf;2* mutants. (n=3, n=1000 grains); (F) Fitted grain filling rate *Nipponbare* (WT) and *cdkf;2* mutants at different stage of grain filling; (G) Fitted grain filling rate *ARF12 OE* transgenic plants and *ARF12 OE -cdkf;2* mutants at different stage of grain filling; (H) Cross-sections of the spikelet hulls of *Nipponbare* (WT), *ARF12 OE* transgenic plants, *ARF12 OE -cdkf;2* and *cdkf;2* mutants (Scale bars, 500 μm) and magnified views of the cross-sections of the spikelet hulls of *Nipponbare* (WT), *ARF12 OE* transgenic plants, *ARF12 OE -cdkf;2* and *cdkf;2* mutants (Scale bars, 50 μm); (I) Statistical analysis of cell number at the outer parenchyma layer of the spikelet hulls of *Nipponbare* (WT), *ARF12 OE* transgenic plants, *ARF12 OE -cdkf;2* and *cdkf;2* mutants (n=10). Experiments were repeated three times and data are presented as mean ± SD; Statistical analysis was performed by Student's *t*-test (**, $P<0.01$; *, $P<0.05$).

Figure 7. Proposed model explaining *miR167-OsARF12* module working downstream of *miR159* regulates grain filling and grain size by *OsCDKF;2* in rice. *miR159* is thought to suppress the expression of *miR167* through OsGAMYBL2 binding the promoter of *miR167h*. *OsARF12* is identified as the main target of *miR167* in rice grain filling regulation. OsARF12 is thought to up-regulate the expression of *OsCDKF;2* by directly binding to motif TGTCGG of the *OsCDKF;2* promoter. *OsCDKF;2* targeted by *OsARF12* mediates auxin and BR signals and involves in cell cycle process, resulting in increased grain filling and grain size. Dashed lines

indicate putative signaling pathway.

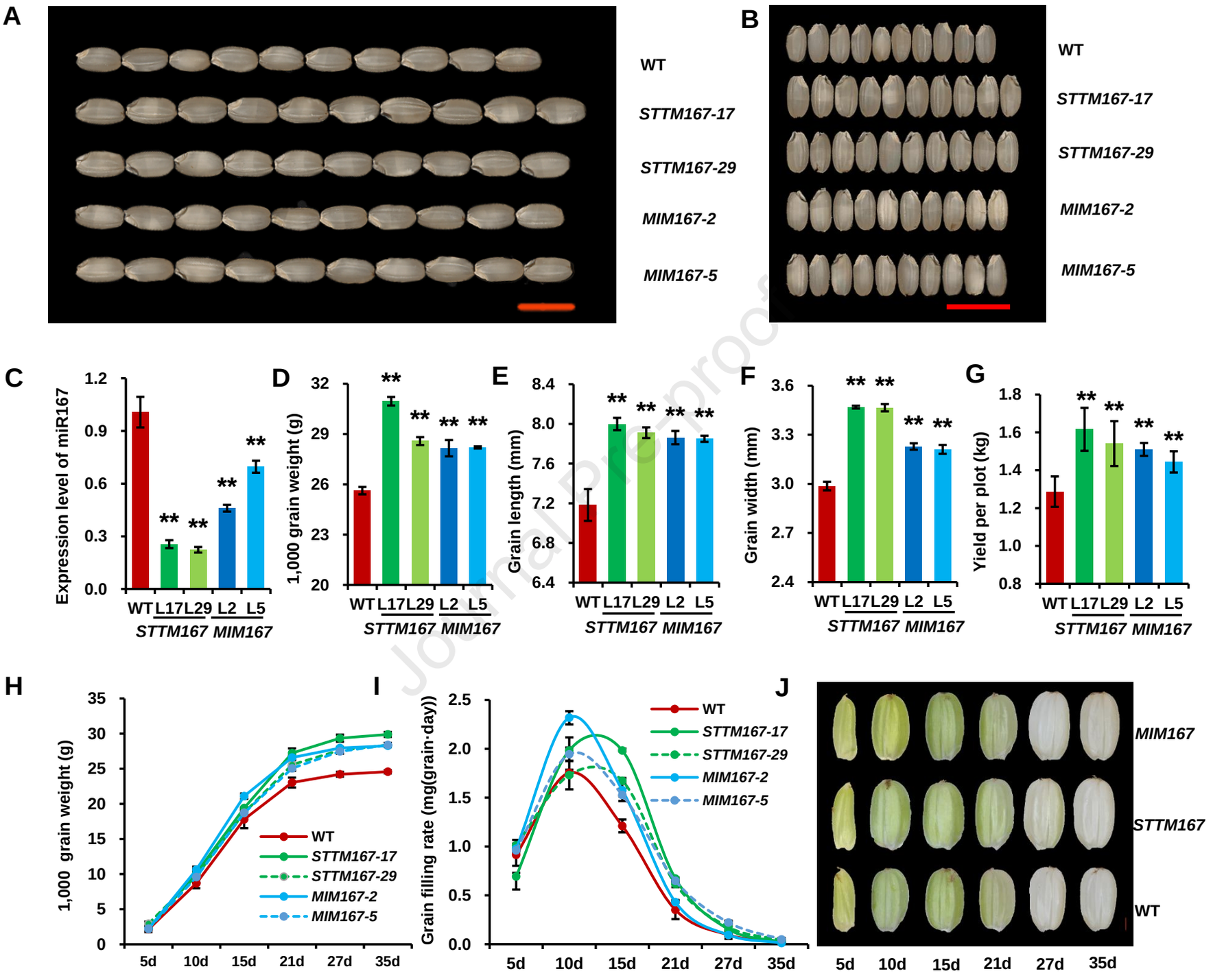
A
WT
STTM167-17
STTM167-29
MIM167-2
MIM167-5
B
WT
STTM167-17
STTM167-29
MIM167-2
MIM167-5
C
Expression level of miR167
D
1,000 grain weight (g)
E
Grain length (mm)
F
Grain width (mm)
G
Yield per plot (kg)
WT L17 L29 L2 L5
STTM167 MIM167
H
1,000 grain weight (g)
I
Grain filling rate (mg(grain·day))
5d 10d 15d 21d 27d 35d
WT
STTM167-17
STTM167-29
MIM167-2
MIM167-5
J
MIM167
STTM167
WT

Figure 1

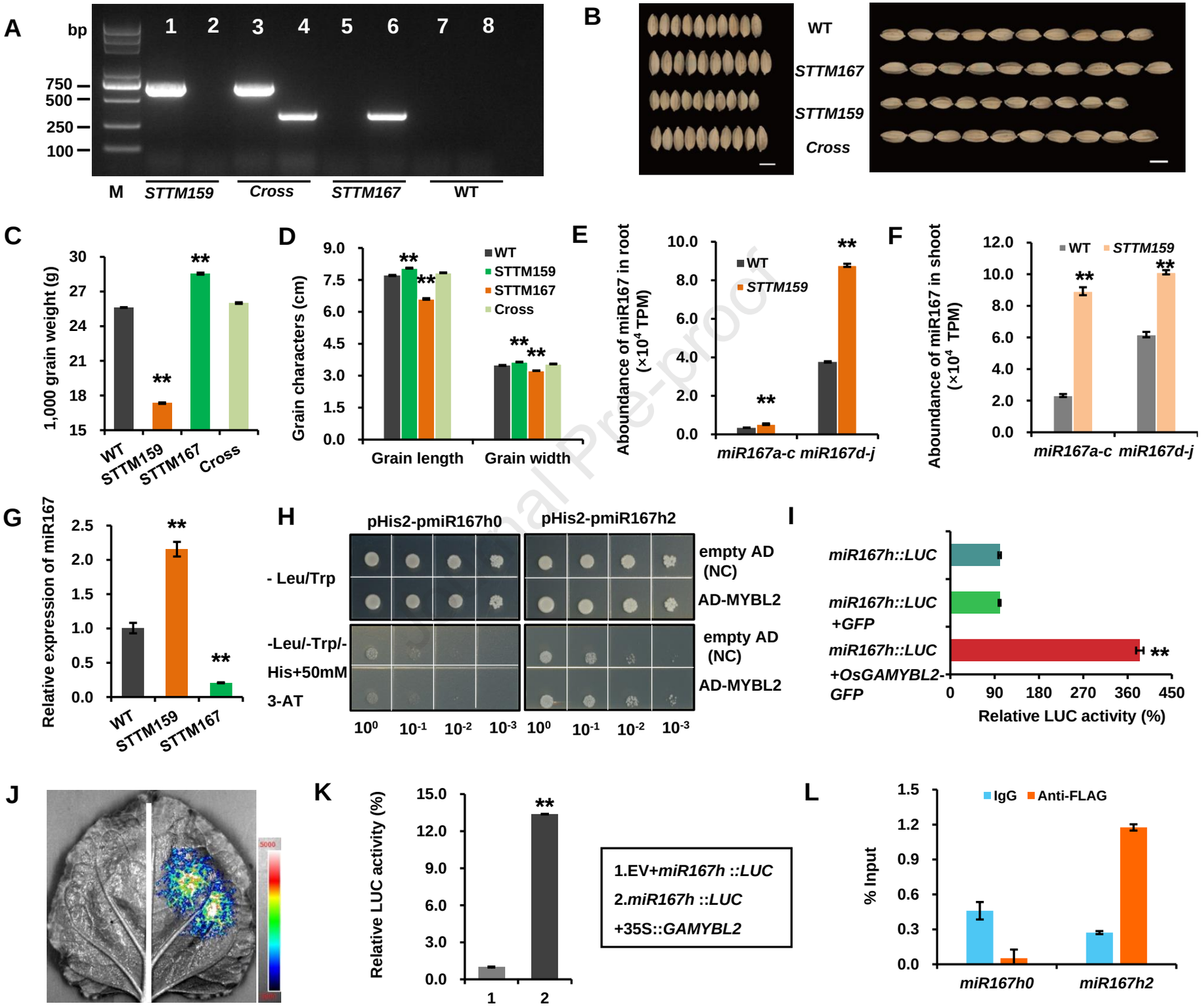

Figure 2

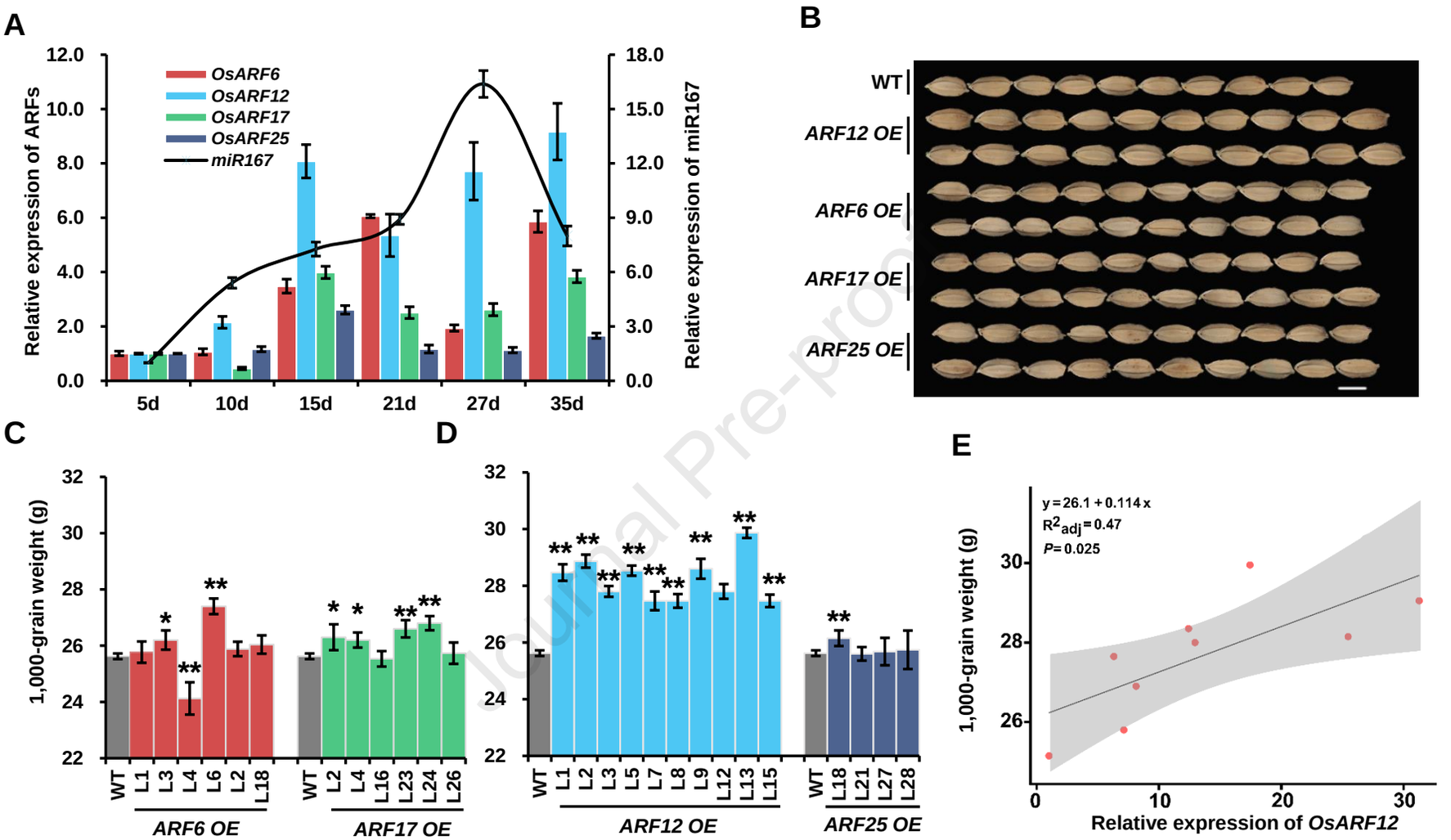
A
Relative expression of ARFs
Relative expression of miR167
OsARF6
OsARF12
OsARF17
OsARF25
miR167
5d
10d
15d
21d
27d
35d
B
WT
ARF12 OE
ARF6 OE
ARF17 OE
ARF25 OE
C
1,000-grain weight (g)
ARF6 OE
ARF17 OE
D
ARF12 OE
ARF25 OE
E
y = 26.1 + 0.114 x
R2adj = 0.47
P = 0.025
1,000-grain weight (g)
Relative expression of OsARF12

Figure 3

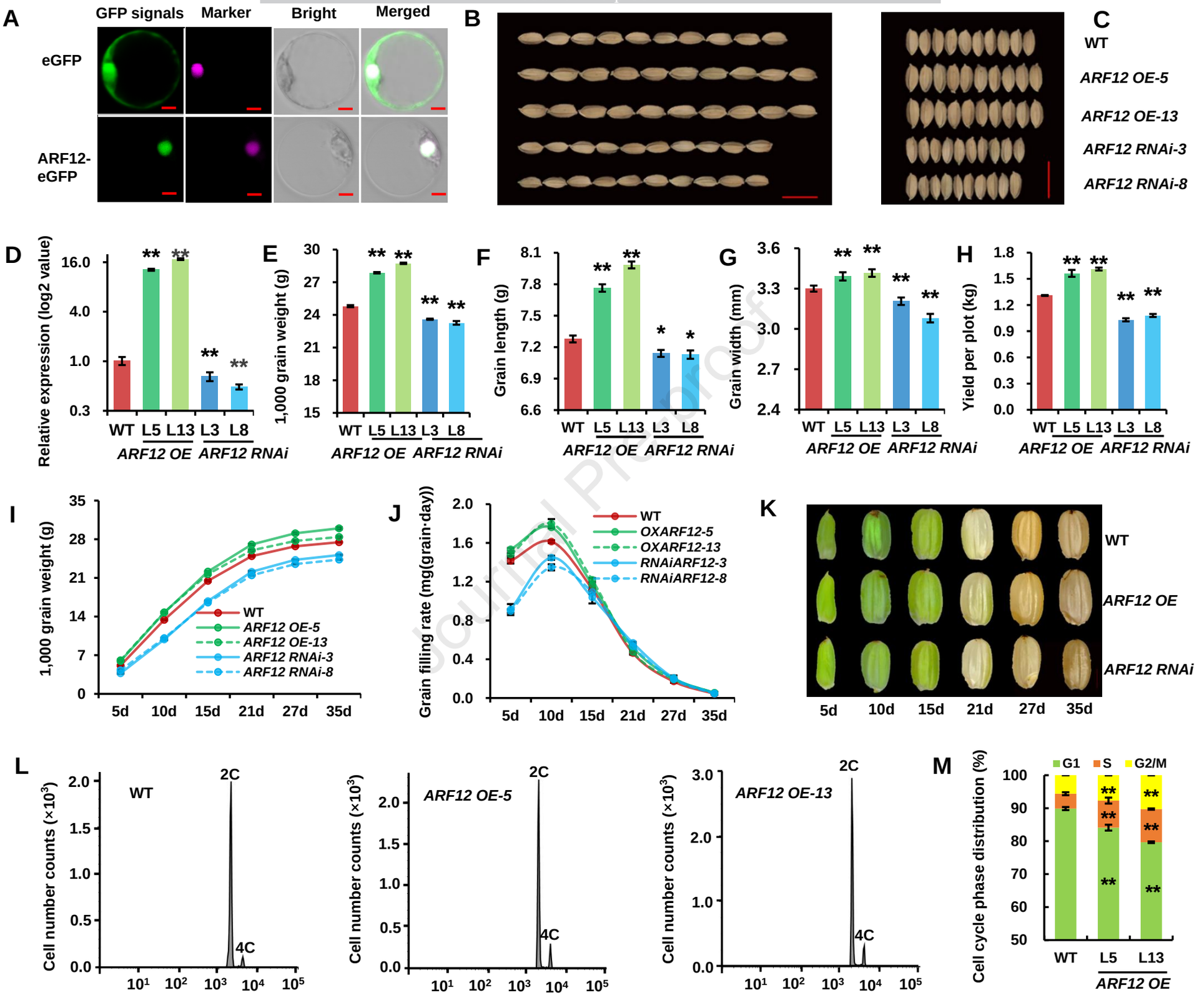

Figure 4

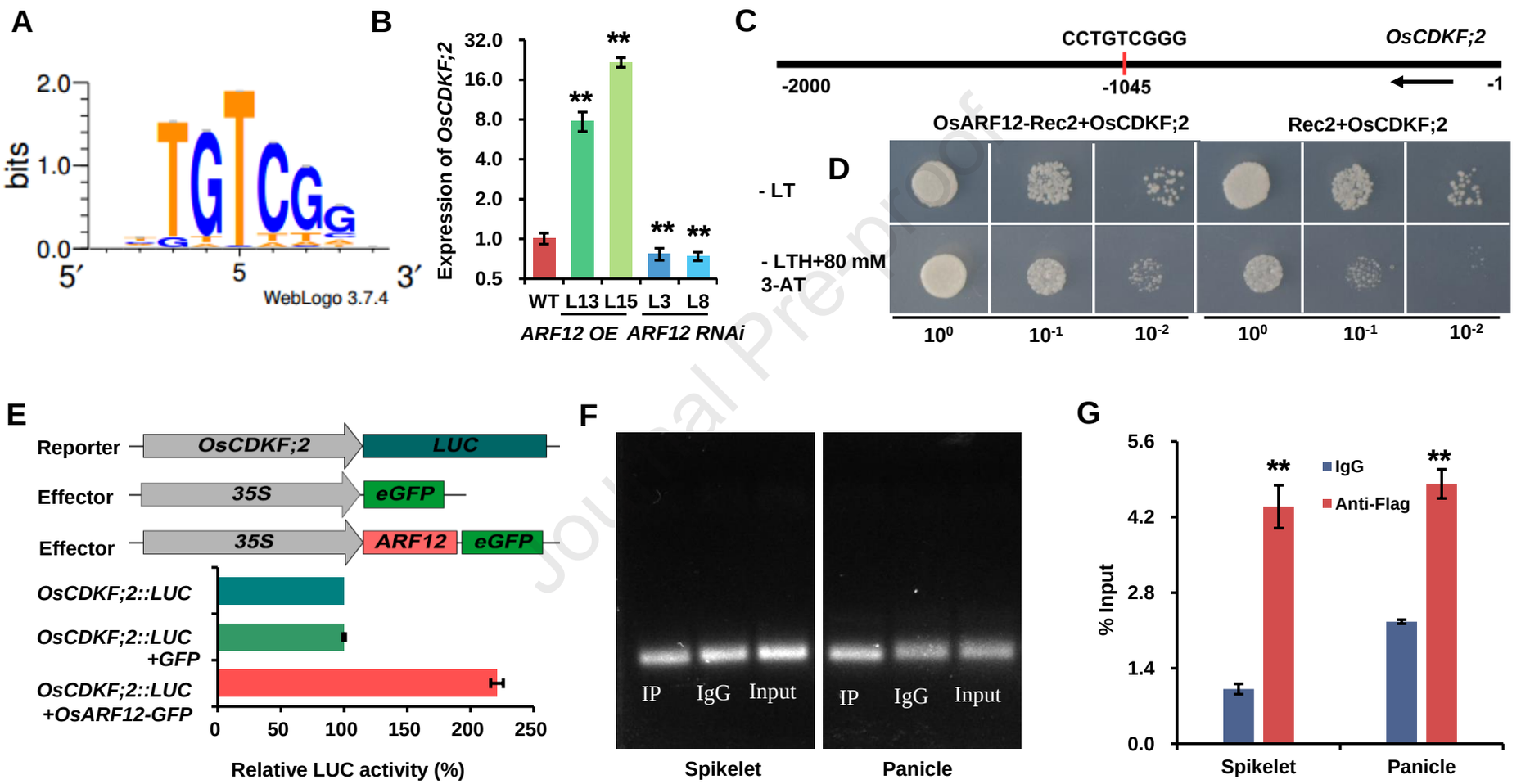
A
2.0
1.0
0.0
bits
5′
5
3′
WebLogo 3.7.4
B
Expression of OsCDKF;2
32.0
16.0
8.0
4.0
2.0
1.0
0.5
**
**
**
**
WT L13 L15 L3 L8
ARF12 OE ARF12 RNAi
C
CCTGTCGGG
OsCDKF;2
-2000
-1045
-1
D
OsARF12-Rec2+OsCDKF;2
Rec2+OsCDKF;2
- LT
- LTH+80 mM 3-AT
10^0 10^-1 10^-2 10^0 10^-1 10^-2
E
Reporter
OsCDKF;2
LUC
Effector
35S
eGFP
Effector
35S
ARF12
eGFP
OsCDKF;2::LUC
OsCDKF;2::LUC +GFP
OsCDKF;2::LUC +OsARF12-GFP
0 50 100 150 200 250
Relative LUC activity (%)
F
IP IgG Input
IP IgG Input
Spikelet
Panicle
G
5.6
4.2
2.8
1.4
0.0
% Input
**
**
IgG
Anti-Flag
Spikelet
Panicle

Figure 5

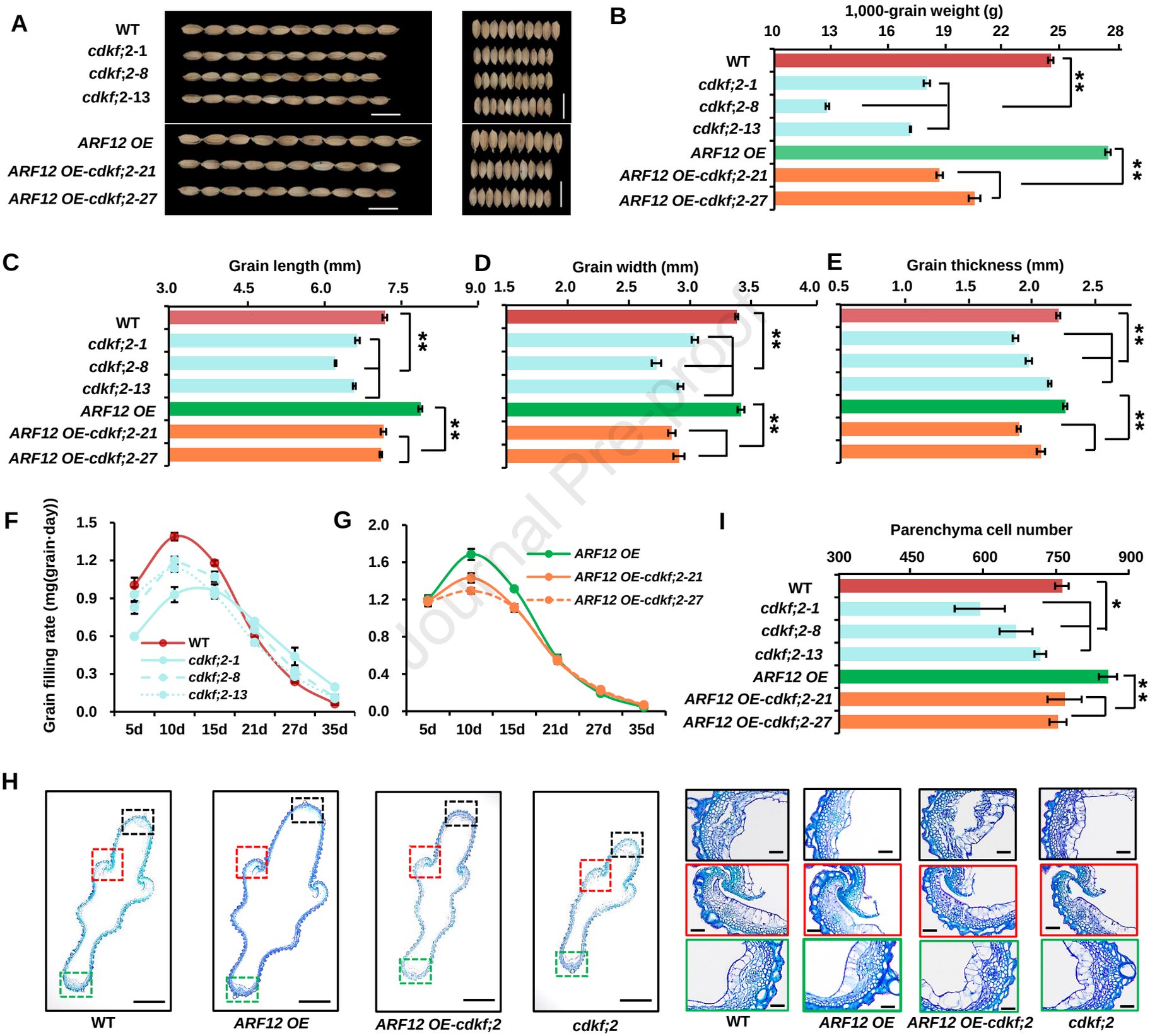

Figure 6

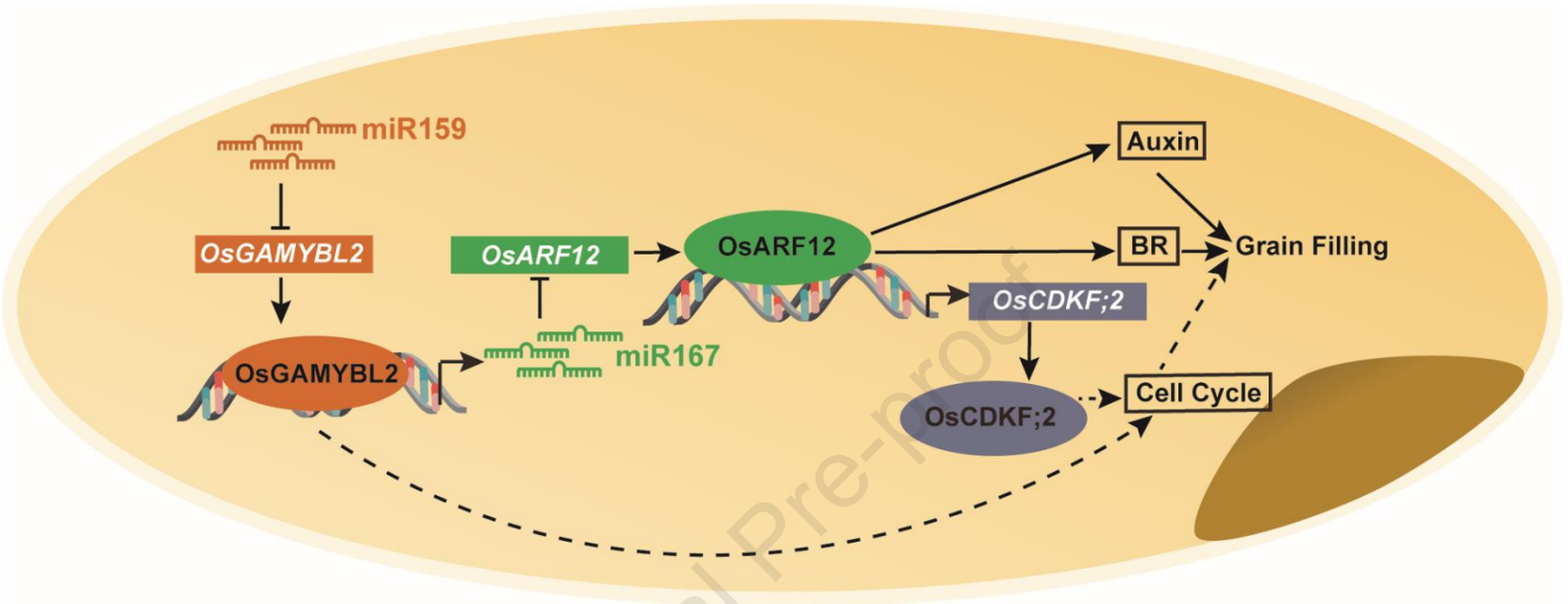

Figure 7